UNIVERSITY OF BORÅS
SCHOOL OF ENGINEERING

Bioremediation of textile dyes and improvement of plant growth by marine bacteria

Pandu krishna Compala prabhakar

This thesis comprises 30 ECTS credits and is a compulsory part in the Master of Science with a Major in Resourse Recovery – Industrial Biotechnology, 120 ECTS credits
No. 11/2012

Bioremediation of textile dyes and improvement of plant growth by marine bacteria

Pandu Krishna Compala prabhakar, s104479@student.hb.se

Master thesis

Subject Category: Technology

University of Borås
School of Engineering
SE-501 90 BORÅS
Telephone +46 033 435 4640

Examiner:	Dr. Elisabeth Feuk Lagerstedt
Supervisor,name:	Dr. M. Jayaprakashvel
Supervisor,address:	Department of Biotechnology, AMET University.
	Chennai-603112, India.
Client:	Department of Biotechnology, AMET University, Chennai.
Date:	2013-01-18
Keywords:	Bioremediation, textile dyes, marine bacteria

ACKNOWLEDGEMENT

This thesis work was a challenging journey in my life. I am very much grateful to all the people who helped me in successfully completing this project work.

I would like to thank Peter Therning and Elisabeth Feuk-Lagerstedt for accepting this thesis project. A special thanks to Dr. Elisabeth Feuk-Lagerstedt for reading this thesis work as an examiner and for her patience, politeness and tolerance.

I am grateful to Prof. Dr. A. Jaffar Hussain, Special officer and Dean, Life Science, AMET University for providing me an opportunity to do this project work in this institution. I express my heartfelt thanks to my Supervisor Dr. M. Jayaprakashvel, Asst. Professor and HEAD, Dept. of Biotechnology, AMET University for his guidance and support during the project. His interest in research was a hugh source of inspiration. I also thank Dr. R.Muthezhilan, Assistant Professor, Department of Biotechnology, AMET University for his guidance and encouragement.

I am indebted to Dr. P. Arumugam and Dr. E. Sagadevan, Armats Biotek for allowing me to use their lab facility. I also thank M. Sridharan for helping me out with FTIR analysis. I am thankful to Venkatramani, Reasearch scholar and all the M.Sc students, especially Prasanth and Vinoth for their support and assistance in the laboratory.

Last but not the least I would like to express my deepest gratitude to my parents and friends. Everything was possible only by their support and prayers.

Thank you all.

ABSTRACT

Textile industries are the major users of dyes in the world. A huge fraction of dyes are discharged out from the textile industries, causing serious damage to the environment. Bioremediation based technologies has been proved to be the most desirable and cost-effective method to counter textile dye pollution. The ability of the microorganisms to decolorize and metabolize dyes can be employed to treat the environment polluted by textile dyes. In this work, a total of 84 bacterial strains were isolated from Kelambakkam Solar Salt Crystallizer ponds (or salterns) and screened for their ability to produce extracellular tannase and laccase enzymes and eventually to decolorize three widely used textile dyes- Reactive Blue 81, Reactive Red 111 and Reactive Yellow 44. Of these 84 strains, 18 strains exhibited tannase activity and 36 strains showed positive laccase enzyme activity. The 11 bacterial strains that displayed both tannase and laccase enzyme activity were screened for their ability to decolorize the three textile azo dyes (100 mg/L). Out of 11 strains only 2 strains *i.e.,* AMETH72 and AMETH77 showed best decolorization (%) in all the three dyes under static condition at room temperature. Repeated- batch immobilization study used to select the most efficient bacterial strain revealed that, isolate AMETH72 was efficient than AMETH77 in decolorizing the dyes. The 16S rRNA sequencing of AMETH72 showed 99% phylogenetic similarity to *Halomonas elongata*. The dye degradation products analyzed by FTIR and UV-Vis techniques displayed complete disruption of azo linkages and biodegradation of dyes to simpler compounds. The treated dyes also improved growth and total chlorophyll content in Wheat and Green gram seedlings, as compared to the untreated dyes. This indicated the non-toxicity of the biologically degraded dye products. Thus the entire study concluded that halotolerant marine bacteria from the salterns can be effectively used to bioremediate the textile dyes.

Keywords: Bioremediation, textile dyes, laccase, immobilization, marine bacteria.

CONTENTS

1 INTRODUCTION 1
1.1 General Introduction 1
1.2 Impact of Textile Dyes 2
1.3 Bioremediation Strategies 3
1.3.1 Microbial degradation of dyes 3
1.3.2 Aerobic and anaerobic degradation of dyes 4
1.3.3 Immobilized cells for degradation of dyes 4
1.4 Role of Enzymes in Dye Degradation 5
1.5 Potential of Marine Microorganisms 5
2 OBJECTIVES 6
3 MATERIALS AND METHODS 6
3.1 Collection of Samples 6
3.2 Isolation of Halotolerant bacteria 6
3.3 Purification and storage of bacterial strains 6
3.4 Screening of bacterial strains for production of tannase enzyme 6
3.5 Screening of bacterial strains for production of laccase enzyme 7
3.6 Screening of selected bacterial strains for decolorization of textile dyes 7
3.6.1 Reactive blue 81 7
3.6.2 Reactive red 111 8
3.6.3 Reactive yellow 44 8
3.7 Immobilization of efficient bacterial strains for decolorization of textile dyes 8
3.8 Analytical methods 9
3.8.1 UV- Visible Spectrophotometric analysis 9
3.8.2 FTIR analysis 9
3.9 Evaluation of bioremediation potential of the efficient bacterial strain 9
3.9.1 Seed germination study (Plate assay) 10
3.9.2 Seedling growth study (Pot assay) 10
3.9.3 Effect of degraded dye on physiochemical parameters of crop plant seedling. 10
3.10 Identification of the efficient bacterial strain AMETH72 11
3.10.1 Gram staining 11
3.10.2 Motility test 11
3.10.3 Endospore staining 12
3.10.4 Catalase test 12
3.10.5 Oxidase test 12
3.10.6 16S rRNA sequencing 12
4 RESULTS 13
4.1 Sample collection and isolation of halotolerant bateria 13
4.2 Screening of bacterial strains for production of tannase and laccase enzyme 13
4.3 Screening of selected bacterial strains for decolorization of textile dyes 13
4.4 Immobilization of efficient bacterial strains for decolorization of textile dyes 14
4.5 Analytical methods 14
4.5.1 UV- Vis analysis 14
4.5.2 FTIR analysis 18
4.6 Evaluation of bioremediation potential of the efficient bacterial strain 22
4.6.1 Seed germination study (Plate assay) 22
4.6.2 Seedling growth study (Pot assay) 23
4.6.3 Effect of degraded dye on physiochemical parameters of crop plant seedlings 24

4.7 Identification of efficient bacterial strain AMETH72 26
5 DISCUSSION 26
6 CONCLUSION 29
7 REFERENCES 30
8 APPENDIX 1 35
9 APPENDIX 2 43
10 APPENDIX 3 48

LIST OF ABBREVIATIONS

HA	Halophilic Agar
HB	Halophilic Broth
FDA	Food and Drug Administration
LiP	Lignin Peroxidase
MnP	Manganese Peroxidase
AMETH	AMET Halotolerant
RB81	Reactive Blue 81
RR111	Reactive Red 111
RY44	Reactive Yellow 44
CW	Control Wheat
BTW	Treated Reactive Blue81 in Wheat
RTW	Treated Reactive Red111 in Wheat
YTW	Treated Reactive Yellow44 in Wheat
BUW	Untreated Reactive Blue81 in Wheat
RUW	Untreated Reactive Red111 in Wheat
YUW	Untreated Reactive Yellow44 in Wheat
CG	Control Green gram
BTG	Treated Reactive Blue81 in Green gram
RTG	Treated Reactive Red111 in Green gram
YTG	Treated Reactive Yellow44 in Green gram
BUG	Untreated Reactive Blue81 in Green gram
RUG	Untreated Reactive Red111 in Green gram
YUG	Untreated Reactive Yellow44 in Green gram
FTIR	Fourier Transform Infrared Spectroscopy
BSA	Bovine Serum Albumin

1 INTRODUCTION

1.1 General Introduction

The textile industry covers two-third of the gross dye stuff market. During manufacturing and usage, approximately 10- 15% of the dye is lost directly to wastewater that finds its way into the environment (Elisangela et al., 2009; He et al., 2004). Color present in the industrial effluent gives a direct indication that the water is polluted. Hence color is the first contaminant recognised in the textile effluent and it has to be removed before discharging into rivers (Khadijah.O, 2009).

Water is a huge resource on earth. Of all the water resources on earth, only 3% of it is not salty and two- third of fresh water exists in the form of glaciers and ice caps. Textile industries are usually located in places near to the sea, mainly for easy overseas transportation. However, the toxic effluents released by the industries causes a great challenge to the marine life. In a year, about 280,000 tonnes of textile dyes are let out into the environment worldwide (Jin et al., 2007) most of which end up into the marine environment. The textile dyes profoundly disturbs the marine ecosystem, as they undergo chemical and biological changes. Their breakdown products might also be toxic to some aquatic organisms. It also greatly affect the photosynthesis of some hydrophytes by limiting light penetration, thereby deteriorating gas solubility and water quality (Shertate and Thorat, 2012).

In present days, reactive dyes are the most widely used dyes because of their broad variety of color shades, brilliant color, ease of application, minimal energy consumption etc. They include chemically different groups. The most common ones are azo, anthraquinone and phthalocyanine dyes (Axelsson et al., 2006). Among these, azo dye constitutes the largest class of synthetic dyes used exhaustively in commercial applications like textile, dying and paper printing. Azo dyes have one or more (-N=N-) groups. They are aromatic hydrocarbons, derivatives of benzene, naphthalene, phenol, toluene and aniline. Decolorization and degradation of textile effluents have been a major environmental concern for a long time. Most of the present research is focused on the degradation of azo dyes which is the one most widely used. The biodegradation of other commercial dyes like phthalocyanines have also been recently addressed (Kirby et al., 2000).

In the past few decades, there is an immense effort to develop a cost-effective and eco-friendly alternative to conventional waste treatment methods. Among all the technologies bioremediation has emerged as the most desirable approach to clean up the environment and to restore its original status. The progressive worldwide adoption of industrial based lifestyle has obviously resulted in anthropogenic impact on the environment. In a motive to improve human standard of living and fashion, textile industries have adopted various new processes that release hazardous substances at various levels of operation. Such an apathy for the environment is a great paradox and can reverse the standard of living by adverse effect on the environment (Shertate and Thorat, 2012).

The bioremediation of textile dyes in marine/ salty environment works well if the indigenous microbes are employed. In other words, halotolerant and halophilic bacteria which can grow well under harsh salty conditions can be applied for bioremediation of textile dyes. Moreover the application of non- indigenous microorganisms might have some deleterious effect on the ecosystem, therefore applying and activating the native microflora is more preferred. Halophilic and halotolerant bacteria are also applied in bioremediation of oil pollution and they are observed to tolerate considerable amount of toxic metals. However, study on their effectiveness for decolorizing textile dye is limited (Asad et al., 2007).

1.2 Impact of Textile Dyes

The wastewater effluent from the textile industry is considered as one of the most polluting among all other industries. The environmental and health effects of textile industry waste water have been a subject to scientific scrutiny for a long time. The chemical nature of the waste from textile industry ranges from organochloride based waste pesticides to heavy metals associated with dyes and dying process (Correia et al., 1994; Faraco et al., 2009).

The disposal of reactive dyes into the environment causes serious damage as they intensely affect the photosynthetic activity of hydrophytes by limiting the light penetration and their breakdown products may be toxic to some aquatic organisms (Wang et al., 2009). It also affects water bodies, ecosystem integrity, soil fertility and plant growth. The azo dyes are becoming a great concern due to their visible color, biorecalcitrance and toxicity to animals and humans (Senan and Abraham, 2004). The microbial metabolic cleavage of azo linkages in the azo dyes results in free aromatic amines that are possibly are toxic, mutagenic or carcinogenic and cause serious health hazard in many life forms (He et al., 2004; Khadijah.O, 2009).

The colored effluents that enter into the water bodies can also cause water- borne disorders such as nausea, perforation of nasal septum, ulceration of skin and mucous membrane, renal damage, cramps, dermatitis, haemorrhage, hypertension, sporadic fever, severe irritation of respiratory tract or cancer. The bioaccumulation of the dyes depends on the availability and persistence in water and food and physiochemical properties (Arun Kumar, 2011; D. Mubarak Ali, 2011).

In the year 1991, FDA certified the use of 3,000 tons of azo dyes in Food, Drugs and Cosmetics. Some of the azo dyes induce liver nodules in experimental laboratory animals. The dye workers have elevated chance of being affected by bladder cancer if exposed to large amounts of azo dyes. Benzidine based azo dyes are widely used by industries. In 1980, The National Institute for Occupational Safety and Health (NIOSH) in US presented a survey data on Benzidine based dyes on laboratory animals and epidemiological studies on dye workers. Benzidine is known to be associated with human urinary bladder cancer and tumorigenic to animals. Administration of benzidine and benzidine congener dyes to experimental animals (rats, dogs and hamsters) showed presence of potentially carcinogenic aromatic amines and their N-acetylated derivative in their urine (Puvaneswari et al., 2006).

The effluent from the textile industry badly affects soil fertility, plant growth and productivity of plants and susceptibility of plants to pathogens. Some parameters for testing plant response to pollutants are germination percentage, seedling survival, shoot and root length of the seedling etc.(Saxena et al., 1986; Singh et al., 2006). Chlorophyll content of the plants also decreases in effect to textile industry effluent. The decrease in total protein, carbohydrates and chlorophyll level is a clear indication of textile dye effluents to be toxic (Puvaneswari et al., 2006).

1.3 Bioremediation Strategies

The general strategy for bioremediation is to boost up the native microorganisms to improve its degradation capacity. However, azo dyes are generally xenobiotic and its degradation is rather difficult. Aerobic degradation of azo dyes is highly preferred. Anaerobic treatment of azo dyes produces by-products such as aromatic amines which are toxic and carcinogenic (Senan and Abraham, 2004)

The removal of color from textile industry effluents are mainly based on physical and chemical methods (Banat et al., 1996). The color removal techniques usually followed in these methods are coagulation or adsorption of dyes, ultra-filtration, ion-exchange, chemical oxidation, electrolysis etc. However these methods are not very much applied because of their high cost, high energy requirements and hazardous by-products. Also these techniques generate a huge volume of sludge and cause secondary pollution due to the formation of sludge and hazardous by-products (Maier et al., 2004; Mohandass Ramya et al., 2007)

Nearly 90% of the reactive textile dyes that enter into the sewage treatment plant, comes out unchanged and discharged into the water bodies (Pierce, 1994). Some azo dyes are difficult to remove because of their high water solubility and low exhaustion (He et al., 2004). The literature suggests that microbial decolorization systems are far more superior in decolorizing textile dyes with total decolorization in just few hours (Balan and Monteiro, 2001)

1.3.1 Microbial degradation of dyes

Microorganisms like bacteria, actinomycetes, fungi and algae have been shown to degrade and biotransform azo dyes (Banat et al., 1996)**.** Fungi and algae have been successful employed in dye decolorization. White rot edible mushroom can grow efficiently on sludge and produce large amount of laccase that reduce the toxicity of the sludge. However, moderate decolorization rate, complexity of textile effluents and long growth cycle limits the performance of fungal systems. In contrast, bacteria are known to degrade and mineralize many reactive azo dyes faster. The intermediate products synthesised during dye decolorization can also de degraded by hydroxylase and oxygenase produced by the bacteria (Banat et al., 1996; Elisangela et al., 2009; Wang et al., 2009)

The azo dyes structures are reductively cleaved into colorless amines by several bacterial species. This behaviour is often seen in aerobic bacteria that grow in the presence of azo compounds.(D. Mubarak Ali, 2011). The intermediate sulfonated amines formed in this process may be aerobically degraded.

The textile industries use sulfonated azo compounds for dying. The degradation of SO_3H containing compounds as substituent is rather difficult to degrade under anaerobic condition. It is shown that a mixed culture of aerobically grown bacteria in 6- aminonaphthalene-2-sulfonic acid is capable of reducing sulfonated azo dyes. Mixed cultures of *Pseudomonas aeruginosa* 3MT and *Pseudomonas sp.* CP4 uses ortho and meta ring cleavage pathway to degrade mixtures of 3-chlorobenzoate and phenols(Babu et al., 1995). *Pseudomonas sp.* CPE1 can completely mineralize 4-Chlorobiphenyl via 4-chlorobenzoate. Some compounds such as chlorobenzenes, chloroanilines and polyaromatic hydrocarbons prevent microbial degradation of dyes, as they get adsorbed to clay and organic matter. (Puvaneswari et al., 2006)

1.3.2 Aerobic and anaerobic degradation of dyes

In reference to the available literature, the microbial degradation of textile dyes is more effective under anaerobic condition. However, toxic aromatic amines are formed at the end of anaerobic process, which could only be degraded by microbes under aerobic conditions. In this context, it has been suggested to combine the anaerobic cleavage of azo dyes with aerobic treatment system for degradation of amines formed. In other words, a sequenced anaerobic/ aerobic biological treatment of textile dye effluents by microbial consortia is suggested in the literature (Banat et al., 1996; Elisangela et al., 2009).

In 2004, Senan and Abraham, developed aerobic bacterial consortium consisting of two isolated strains BF1, BF2 of *Pseudomonas* and *Pseudomonas putida* MTCC1194 for aerobic degradation of mixture of azo dyes. The analysis of degradation products showed that the dye was converted to low molecular weight compounds (Senan and Abraham, 2004).

1.3.3 Immobilized cells for degradation of dyes

In recent times many bioreactor designs have been developed for the anaerobic/aerobic treatment of textile dyes. Some of them are packed bed bioreactors, fixed film bioreactors, aerobic suspended- bed activated sludge bioreactor, pulse flow bioreactors, anaerobic/aerobic rotating biological contractors and anaerobic up-flow fixed bed column with an aerobic agitated tank, etc. Many have reported that continuous decolorization of many dyes are efficiently done in rotating biological reactors and packed bed bioreactors.

Immobilization of microbial cells is a best way to exploit their ability to degrade textile dyes. It has many advantages than a free cell. It prevents cell washout and a high cell density to be maintained in bioreactors. The catalytic stability of microbes is often improved by immobilization. This enables the microbial cells to degrade high concentration of toxic compounds. Immobilization also enhances substrate uptake as there is ample amount of nutrient available at the solid- liquid interface. Immobilised *Pseudomonas putida* P8 cells degraded catechol more efficiently than their free cell counterparts. It also showed efficient degradation of nitriles, by utilizing acetonitrile as a source of carbon and nitrogen (Puvaneswari et al., 2006).

1.4 Role of Enzymes in Dye Degradation

Enzymes are the ultimate molecules which deal with the dye compounds and bring about cleavage and successive degradation. The initial step in degrading the azo dye is to cleave the electrophilic azo linkage, which immediately causes decolorization. Azoreductase brings about the cleavage of azo linkages in compounds containing azo bond to produce aromatic amines. Many bacterial strains have been found to contain unspecific cytoplasmic enzymes that act as azoreductase.

The mammals can synthesize azoreductase (called as hepatic azoreductase) in their body. In mammals the hepatic azoreductase and the bacterial azoreductase can breakdown the azo dyes to their corresponding amines. However, bacterial azoreductase are more active than hepatic azoreductase in doing the job and reduces the azo dyes to mutagenic and carcinogenic amines (Puvaneswari et al., 2006).

The phenoloxidases namely lignin peroxidase (LiP), manganese peroxidase (MnP) and laccase has a great potential to degrade many aromatic compounds. These enzymes are involved in degradation of lignin, which are complex polyaromatic polymers. Laccases (benzenediol: oxidoreductase; EC 1.10.3.2) belong to the class oxidoreductase- a multicopper oxidase family, which can oxidise phenols, polyphenols and aniline by one- electron abstraction. MnP belongs to the class of peroxidase. It can only act on phenolic substrates using Mn^{2+}/ Mn^{3+} as an intermediate redox couple, while LiP prefers non- phenolic methoxy substituted lignin subunits as substrates (Abadulla et al., 2000). Tannase (Tannin acyl hydrolyase, EC 3.1.1.20) is a ligninolytic enzyme that acts on carboxylic ester bonds. It catalysis the hydrolysis of central ester bonds between two aromatic rings of digallate. It is a key enzyme in the degradation of gallotannins which is hydrolysable tannin. Tannin or tannic acid is polyphenolic compound which have sufficient hydroxyl and carboxyl groups to form a strong complex with proteins and other macromolecules. Tannic acids are widely used as mordant in dying process for cellulose fibre such as cotton (McMullan et al., 2001).

1.5 Potential of Marine Microorganisms

Marine microbes are those microscopic organisms that are generally found in saltwater. These microorganisms fall into the category of viruses, bacteria, protista groups which differs greatly in their biological characteristics. The ecological role they play is profound. They form the base of the food chain in marine environment. The marine environment has abundance of potentially active biomolecules which are yet to be explored.

Facultative and obligate marine fungi namely *Sordaria fimicola, Flavodon flavus, Algialis grandis, Hypoxylon oceanicum* have been studied to decolorize dyes. In bacteria, *Pseudomonas fluorescens, Pseudomonas aeruginosa, Bacillus cereus, Proteus vulgaris, Bacillus subtilis, Acenetobacter sp., Zooglea sp.* are known to decolorize dyes. Marine fungi isolated from decaying mangrove wood, leaves, sea grass has the ability to degrade and reminiralize lignocellulosic substrates by using their extracellular lignin degrading enzymes. The marine microbes are useful in dye degradation mainly because they can survive the harsh

saline conditions of the textile dye effluent. Their enzyme system can function efficiently in neutral/ alkaline pH and wide range of temperatures to act on varying neutral/alkaline textile dye effluents (Shertate and Thorat, 2012).

2 OBJECTIVES

The objective of this work is to identify a marine bacterium which is highly efficient in degrading some of the azo dyes widely used in the textile industry. This thesis work also focuses on the plant growth promotion by the biologically degraded dye products.

3 MATERIALS AND METHODS

3.1 Collection of Samples

The soil samples were collected from the nearby Kelambakkam Solar Salt Crystalliser ponds, Tamil nadu, India (Latitude 12.78, Longitude 80.23). The samples were collected from both the soil surface and from the rhizosphere of halophytes growing on the saltern region. The samples were sorted into two groups- rhizosphere soil and non-rhizosphere soil. The soil samples were transferred into sterile plastic bags and taken to laboratory immediately.

3.2 Isolation of Halotolerant bacteria

10 g of soil sample was taken in sterile conical flasks and 99 ml of sterile distilled water was added to each flask. The flasks were kept in shaker for approximately 15 minutes at 100 rpm. This 10^{-1} master dilution was serial diluted upto 10^{-3} dilution. Then 0.1 ml from 10^{-3} dilution was used to spread plate on 3% Halophilic Agar (HA) medium (Appendix 1, Table 1). The plates were left for overnight incubation at 37^{o}C.

3.3 Purification and storage of bacterial strains

After incubating the plates for 24 hours, bacterial colonies were seen. The colony morphology of the isolated bacterial colonies was noted. The bacterial strains were isolated and sub-cultured on 3% HA plates. The bacterial strains were sub-cultured every week by streak plate method. The strains were given accession numbers with prefix AMETH meaning AMET Halotolerant. The strain numbers were from AMETH 01 to AMETH 84. The bacterial strains were stored in sterile sea water in 1.5 ml eppendorf tubes at 4^{o}C. The bacterial strains were also grown in HA medium with different salinity (0- 12% NaCl).

3.4 Screening of bacterial strains for production of tannase enzyme

Tannic acid acts as a substrate for the production of tannase enzyme. The 3% HA medium and 0.5% tannic acid solution were sterilized separately. The two solutions were mixed together just before pouring into the petri plates. The freshly prepared medium was milky

white in color. The bacterial strains were spot inoculated on the medium (9 bacterial strains per plate) and incubated overnight at room temperature. Tannase producing bacteria shows a dark brown zone around the bacterial culture (Kiiskinen et al., 2004).

3.5 Screening of bacterial strains for production of laccase enzyme

Guaiacol acts as a substrate and indicator compound in the screening of microbes for laccase production. 0.2% of guaiacol was added to 3% HA medium before autoclaving. The cultures were spot inoculated on the medium (9 cultures per plate) and incubated in dark at room temperature. Laccase producing strains shows reddish brown coloration around the culture in a normally colorless medium after four days of incubation (Kiiskinen et al., 2004).

3.6 Screening of selected bacterial strains for decolorization of textile dyes

The tannase and laccase enzyme producing strains were screened for their ability to decolorize three textile dyes namely Reactive blue 81 (RB81), Reactive red 111 (RR111) and Reactive yellow 44 (RY44). Test tubes containing 10 ml of Half- strength 3% Halophilic broth (HB) medium with 100 mg/L of RB81, RR111 and RY44 was prepared and autoclaved. To this a loopful of bacterial culture was inoculated. The tubes were incubated for 9 days under static condition at room temperature. The details of the dyes used are given below.

3.6.1 Reactive blue 81

Generic name: Blue M2R

CI name: Reactive blue 81

CAS registry number: 75030-18-1

Synonyms: 5-[(4, 6-Dichloro-1, 3, 5-triazin-2-yl) amino]-4-hydroxy-3-[2-[4-(phenylamino)-3-sulfophenyl] diazenyl]-2, 7-naphthalenedisulfonic acid sodium salt; Helaktyn Blue F2R.

Molecular formula: $C_{25}H_{17}Cl_2N_7O_{10}S_3^{\cdot}{}_3Na$

Dye type: Azo dye

Structure:

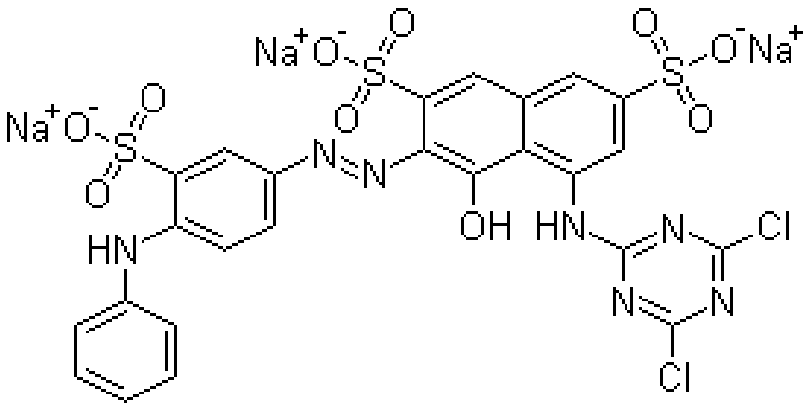

Fig 3.1: Structure of Reactive Blue 81(Chemblink).

3.6.2 Reactive red 111

Generic name: Red BSID

CI name: Reactive red 111

CAS registry number: 88232-20-6

Molecular formula: Unknown

Dye type: Azo dye

Structure: Unknown

3.6.3 Reactive yellow 44

Generic name: Yellow MR

CI name: Reactive yellow 44

CAS registry number: 12270-91-6

Synonyms: Amaryl Yellow R; Reactive Golden Yellow MR.

Molecular formula: Unknown

Dye type: Azo dye

Structure: Unknown

After 9 days of incubation, 4 ml of sample from each tube was removed and centrifuged at 10,000 rpm for 6 minutes at 4^{o}C. The absorbance of the supernatant was measured by ELICO SL159 UV- Visible Spectrophotometer. The absorbance maximum of RB81, RR111 and RY44 was 576 nm, 533 nm and 413 nm respectively. The percentage of decolorization was calculated using the following formula:

$$\% \text{ Decolorization} = \frac{\text{Initial absorbance} - \text{Final absorbance}}{\text{Initial absorbance}} \text{ X } 100$$

3.7 Immobilization of efficient bacterial strains for decolorization of textile dyes

The bacterial strains which had the capacity to efficiently decolorize all the three textile dye were checked for their decolorization capacity when immobilized. The immobilization of cells was performed by using 3% sodium alginate and 0.2 M of calcium chloride. The overnight grown bacterial cells were suspended in 3% sodium alginate. The cells- alginate mixture was dripped into cross- linking solution made of 0.2 M $CaCl_2$ to form calcium alginate beads. The diameter of beads was found to be in the range of 3 mm to 4 mm. The beads were left in the calcium chloride solution for 3 hours to attain desirable hardness.

Repeated- batch immobilization study used to select the most efficient bacterial strain. Varying number of beads (1 bead/ml, 2 beads/ml and 3 beads/ml) was transferred into test tubes containing 10 ml of respective dye (100 mg/L) + 3% HB medium mixture. This was

then incubated for 3 days under static condition at room temperature. It was called Batch #1. The beads were then rinsed twice with sterile distilled water and transferred into respective dye+ medium mixture and incubated for 3 days. This was called Batch #2. The same procedure was repeated upto Batch #6. The incubation period of each Batch was fixed to 3 days. The decolorized supernatant belonging to all the batches were measured for absorbance. The absorbance values were used to calculate percentage of decolorization, as described previously. The bacterial strain that showed the best decolorization ability was concluded to be the most efficient bacterium among all the bacterial isolates of this study. This was followed by few analytical methods and evaluation studies.

3.8 Analytical methods

The immobilized beads of most efficient bacterium were inoculated into 25 ml of medium containing the respective dye and 0.025 g of yeast extract. This was incubated for 9 days in static condition at room temperature. Then the supernatant was obtained by centrifugation at 10,000 rpm for 10 minutes. The respective dye (100 mg/L) solution incubated without beads was taken as control for the dyes. These supernatants were used in the following analysis:

3.8.1 UV- Visible Spectrophotometric analysis

The supernatant of the respective dyes were studied in UV- Vis Spectrophotometer for change in UV- Vis spectra before and after decolorization. 4 ml of the supernatant was taken and absorption spectrum from 200 nm to 700 nm was recorded using UV- Vis spectrophotometer (Shimadzu UV-1700s).

3.8.2 FTIR analysis

FTIR analysis was performed using Shimadzu FTIR- 8400S. A drop was sample was taken and placed on the salt plate. The salt plate was then fixed to the sample holder. The spectra were collected in scanning range of 650- 4000 cm^{-1}. The FTIR was first calibrated for background signal- scanning without any sample (air blank), and then the experimental samples were scanned. The IRsolution software generates reports by subtracting the spectrum of the air blank from the spectrum of the experimental samples.

3.9 Evaluation of bioremediation potential of the efficient bacterial strain

The evaluation of bioremediation potential was done by plant growth promotion studies to determine the toxic nature of the end products of three textile dyes that were decolorized by the most efficient bacterium. Plant growth promotion studies were carried out on two crop plants viz. *Triticum aestivum* (wheat), a monocot and *Vigna radiata* (Green gram), a dicot. In the following text, untreated dye indicates colored dye or the dye that was not treated with the efficient bacterium and treated dye indicates decolorized dye or the dye that was decolorized by the most efficient bacterium.

3.9.1 Seed germination study (Plate assay)

The experiment was done in disposable plastic petri plates. The top and the bottom of the petri plates were padded with a layer of tissue paper. Wheat and green gram seeds (40 each) were soaked in 25 ml of colored/untreated dye and 25 ml of decolorized/treated dye for 6 hours. For the controls, seeds were soaked in water for 6 hours. After soaking 40 seeds were placed in each petri plates and the tissue paper was soaked with their respective dye mixtures. The plates were incubated for 3 days. The tissue paper was kept moist by spraying water. After 3 days the germination percentage was calculated using the following formula:

$$\%\ germination = \frac{\text{number of seeds germinated}}{\text{total number of seeds}} \text{ X } 100$$

3.9.2 Seedling growth study (Pot assay)

Pot experiments were carried out in plastic pots having diameter of 6.5 cm and height of 8 cm. 150 g of sterile red soil was added to each pot. The wheat and green gram seeds (40 each) were soaked in 25 ml of colored/untreated dye mixture and 25 ml of decolorized/treated dye mixture for 6 hours. Suitable controls were made with water. 5 seeds each of wheat and Green gram from every treatment were added to the pots. The seeds were then watered with samples (treated and untreated dye mixture) for the first time. The soil was kept moist by spraying water daily. The shoot length, root length and fresh weight of wheat and Green gram seedlings were recorded after 10 days.

3.9.3 Effect of degraded dye on physiochemical parameters of crop plant seedling

The crop plant seedlings from the Pot assay experiment was used to calculate total carbohydrate, total protein and total chlorophyll content. 0.5 g of crop plant seedling was measured and well grinded with 10 ml of phosphate buffer (Appendix 1, Table 2) for total carbohydrates and protein estimation and with 10 ml of 80% acetone for total chlorophyll estimation using motor and pestle. The mixture was filtered with cloth gauze. The filtrate was then centrifuged at 8000 rpm for 4 minutes at 4^{o}C. This plant extract was collected in sterile tubes and stored in 4^{o}C for the following analysis.

3.9.3.1 Estimation of total carbohydrate content in plant extract

The Phenol- sulfuric acid method was used to estimate the total carbohydrates in the plant extract. To 1 ml of plant extract, 500 µl of 5% phenol and 2.5 ml of conc. sulfuric acid were added. This mixture was incubated in dark for 10 minutes. The absorbance of the samples was measured at 490 nm. The reagent blank was prepared by mixing 1 ml distilled water, 500 µl of 5% phenol and 2.5 ml of conc. sulfuric acid. The standard curve was prepared by using D-glucose. (Sadasivam and Manickam, 1996).

3.9.3.2 Estimation of total protein content in plant extract

The Bradford method was used to estimate the total proteins in the plant extract. 1 ml of plant extract was mixed with 5 ml of Bradford reagent (Appendix 1, Table 3). Then absorbance was

measured at 595 nm using UV- Visible spectrophotometer. The reagent blank was prepared by mixing 1 ml of distilled water with 5 ml of Bradford reagent. The standard curve was prepared by using BSA. (Sadasivam and Manickam, 1996).

3.9.3.3 Estimation of total chlorophyll content in plant extract

1 ml of the plant extract was mixed with 9 ml of 80% acetone and the optical densities were recorded at 663 nm and 645 nm. The total chlorophyll content was estimated by the method of Arnon (Arnon, 1949).

3.10 Identification of the efficient bacterial strain AMETH72

3.10.1 Gram staining

Gram staining is a differential staining method based on difference in cell wall of bacteria.

Procedure

- A thin film smear of bacterial culture was made by heat fixation.
- The slide was flood with crystal violet for a minute.
- Slide was rinsed with tap water by tilting the slide slightly to rinse all the stains from the slide.
- The slide was then flooded with Grams iodine for 1minute and washed gently with tap water.
- Slide was titled slowly and 95% ethanol was dropped until blue color run off the smear. Then the slide was immediately rinsed in water.
- Safranin was then added to the slide and hold for 30 seconds. Then slide was rinsed with water to remove excess stain.
- Slide was put on bibulous paper and gently blotted to remove water.
- The slide was observed under microscope. Generally, cells with violet color are gram positive while cells appearing in pink color are gram negative.

3.10.2 Motility test

Hanging drop technique was used for testing motility of the bacteria.

Procedure:

- A clean cover slip and a cavity slide were taken. The cavity slide was greased at four corners.
- A drop of culture from overnight incubated culture broth was taken with a sterile loop and placed on the centre of cover slip.
- The cavity slide was inverted and placed on the cover slip.
- It was then observed under microscope.

3.10.3 Endospore staining

For endospore staining, the Schaeffer- Fulton method was used.

Procedure:

- A smear of the bacterial culture was made. It was allowed to air dry and heat fix.
- Malachite green stain was applied to the slide and steamed for 5 minutes over a container of boiling water.
- Then the slide was washed with tap water and counterstained by safranin for 30 seconds.
- The slide was examined under oil immersion lens for the presence of endospores. The endospores are generally bright green and the vegetative cells are brownish red/ pink.

3.10.4 Catalase test

Catalase production can be determined by adding Hydrogen peroxide to bacterial cultures. If catalase is present a chemical reaction occurs, indicated by bubbles of free oxygen gas. This is positive catalase test. While absence of gas bubbles indicate negative catalase test.

Procedure:

- A loop full of culture was taken and placed on a clean glass slide.
- A drop of 3% Hydrogen peroxide solution was placed on the bacterial culture and mixed well will sterile loop.

3.10.5 Oxidase test

The oxidase test checks for the presence of indophenol oxidase enzyme. Tetramethyl-para-phenylenediamine (oxidase reagent) will be oxidised in the presence of atmospheric oxygen by indophenol oxidase causing the formation of a dark- purple compound called indophenols.

Procedure:

- The bacterial culture was taken in a sterile loop.
- This was rubbed on the oxidase disc (HIMEDIA®).
- The disc was observed for 10- 30 seconds for development of dark purple color around the edge of the organism. A dark purple color development is taken as positive test and no color development is taken as negative test.

3.10.6 16S rRNA sequencing

The 16S rRNA analysis was used to identify the selected efficient bacterial strain AMETH72. The bacterial strain AMETH72 was sent to Jayagen Biologics, Chennai where the following was performed to identify the bacteria strain. The nearly full-length 16S rRNA gene was

amplified by PCR with Forward primer 5'-AGAGTTTGATCCTGGCTCAG-3' and Reverse primer 5'-ACGGCTACCTTGTTACGACTT-3'. The 16S rRNA amplified fragments were purified using the QIAquick gel extraction kit (Qiagen) from the agarose gel and sequenced using automated DNA sequencer (Model 3100, Applied Biosystems, USA). The sequences were analysed using the Basic Local Alignment Search Tool (BLAST) software (http://www.ncbi.nlm.nih.gov/blast) against the 16S rRNA sequence database.

In the Phylogenetic analysis, the sequences of the 16S rRNA genes were compared against the sequences available from GenBank using the BLASTN program and were aligned using CLUSTAL W software. Distances were calculated according to Kimura's two-parameter correction (Kimura, 1980). Phylogenetic trees were constructed using the Neighbor-joining method. Bootstrap analysis was done based on 1000 replications. The MEGA 5 package was used for all analyses.

4 RESULTS

4.1 Sample collection and isolation of halotolerant bateria

A total of 84 bacterial strains were isolated among which 32 strains belong to Rhizosphere soil and 52 strains belong to Non- rhizosphere soil (Appendix1, Table 5). The colony morphology of the bacterial strains was recorded (Appendix1, Table 6). Some of the isolated colonies were pigmented. However, majority of the colonies were white, small and circular in shape. All the strains were able to grow on HA medium with salinity ranging from 0-12% NaCl. This indicated that the strains were halotolerant bacteria. The strains were sub-cultured on 3% HA medium and preserved.

4.2 Screening of bacterial strains for production of tannase and laccase enzyme

18 strains out of 84 strains showed positive tannase activity. The formation of a dark brown zone around the spot inoculated bacterial culture indicated that the extra-cellular tannase enzyme is produced. The brown coloration was due to the release of gallic acid caused by the hydrolysis of tannic acid by tannase enzyme. 36 strains out of 84 strains showed positive laccase activity. The formation of reddish- brown coloration around the culture indicated the presence of laccase enzyme (Appendix 1, Table 7).

4.3 Screening of selected bacterial strains for decolorization of textile dyes

The bacterial strains that showed positive tannase and laccase activity were screened for their ability to decolorize the textile dyes namely RB81, RR111 and RY44. The percentage of decolorization by 11 bacterial strains is given in Appendix 1, Table 8. From the decolorization data, it was observed that out of 11 bacterial strains only 2 strains, AMETH72 and AMETH77 showed good decolorization in all the 3 reactive dyes. The decolorization of RB81, RR111 by AMETH72 and AMETH77 was observed visually within 24 hours of incubation. However, the decolorization in RY44 was difficult to detect by visual inspection. Although AMETH76

showed good decolorization with RR81, it failed to display good decolorization with RY44. It was seen that majority of the selected bacterial strains decolorized RB81 readily when compared to RR111 and RY44 dyes.

4.4 Immobilization of efficient bacterial strains for decolorization of textile dyes

The two strains AMETH72 and AMETH77 were immobilized and compared for their ability to decolorize the textile dyes. After immobilization, there was a good improvement in decolorization percentage by both the strains, as compared to their free cell counterparts. From the percentage of decolorization chart (Appendix 2) of RB81, RR111 and RY44 it can be seen that AMETH72 decolorizes the dyes better than AMETH77. The percentage of decolorization of AMETH72 in almost all the batches was higher than AMETH77 especially in Batch #1, 2 and 3. The best decolorization for RB81 by AMETH72 was achieved at batch #1 (3 beads/ml) with 97.63% decolorization. The best decolorization for RR111 by AMETH72 was achieved at batch #2 (3 beads/ml) with 89.66% decolorization. The best decolorization for RY111 by AMETH72 was achieved at batch #2 (3 beads/ml) with 85.35% decolorization. The best decolorization for RB81, RR111 and RY44 by AMETH77 was achieved at batch #2 (3 beads/ml) with 96.80%, 88.93% and 83.91% decolorization respectively. Therefore, it was concluded that AMETH72 was the most efficient of all the bacterial strains in decolorizing all the three textile dyes. The decolorization (%) by AMETH72 for all 3 dyes was higher in 3 beads/ml than 2 beads/ml or 1 bead/ml.

4.5 Analytical methods

4.5.1 UV- Vis analysis

The decolorization and degradation of the three azo dyes were studied by UV- Vis analysis. For the untreated dyes in Fig. 4.1, RB81 showed four peaks at 205 nm, 259 nm, 283 nm and 576 nm. In Fig. 4.3, RR111 displayed absorbance peaks at 233.5 nm, 290 nm, 311.5 nm, 374.5 nm and 533 nm. In Fig. 4.5, RY44 presented four peaks at 211.5 nm, 227.5 nm, 311 nm and 413 nm. For all the treated dyes, the absorbance peaks in the visible region disappeared, which indicated complete decolorization (Fig. 4.2, Fig. 4.4 and Fig. 4.6). In the UV spectra, all the peaks that belonged to the untreated dyes disappeared (except for the RY44 absorbance peak at 277.5 nm) and were replaced by several new peaks in the range 203- 368 nm.

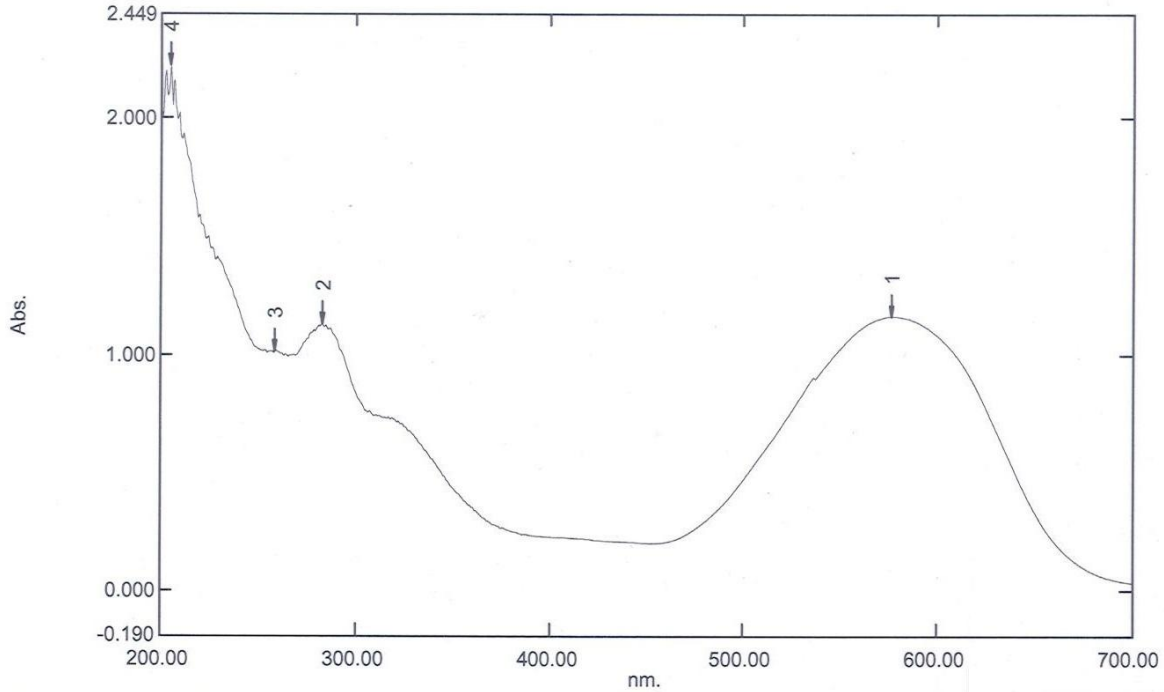

Fig 4.1: UV- Vis spectrum of Reactive Blue 81 before decolorization. X-axis; represents the wavelength (nm). Y-axis; represents the Absorbance.

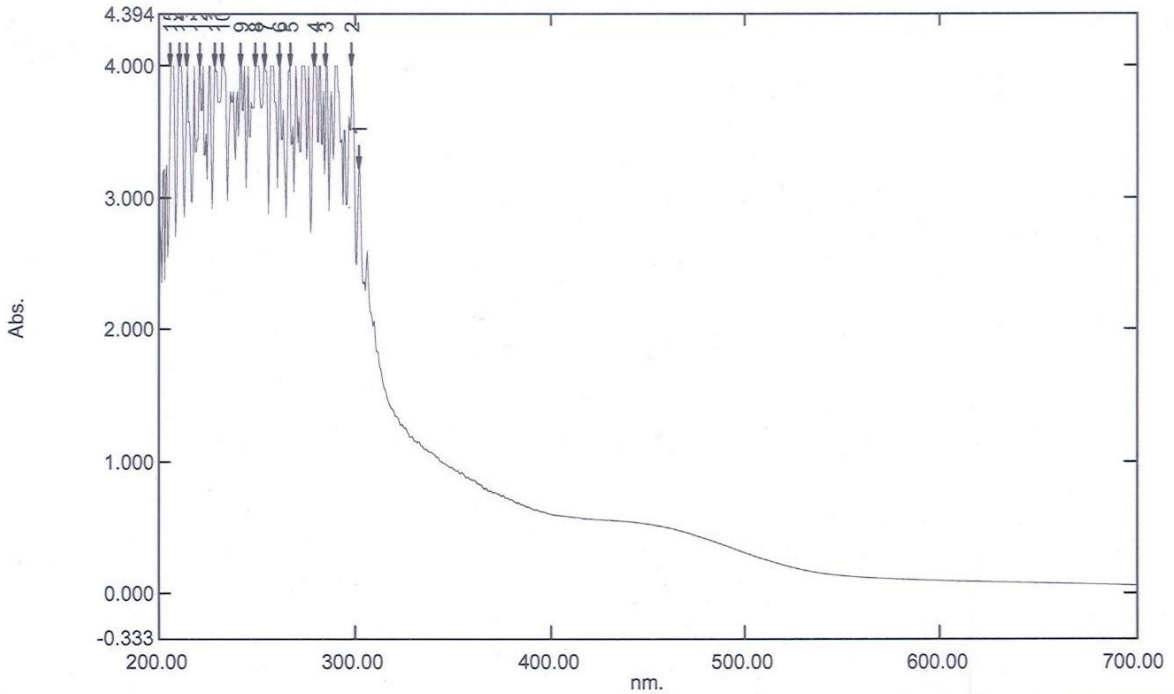

Fig 4.2: UV- Vis spectrum of Reactive blue 81 after decolorization. X-axis; represents the wavelength (nm). Y-axis; represents the Absorbance.

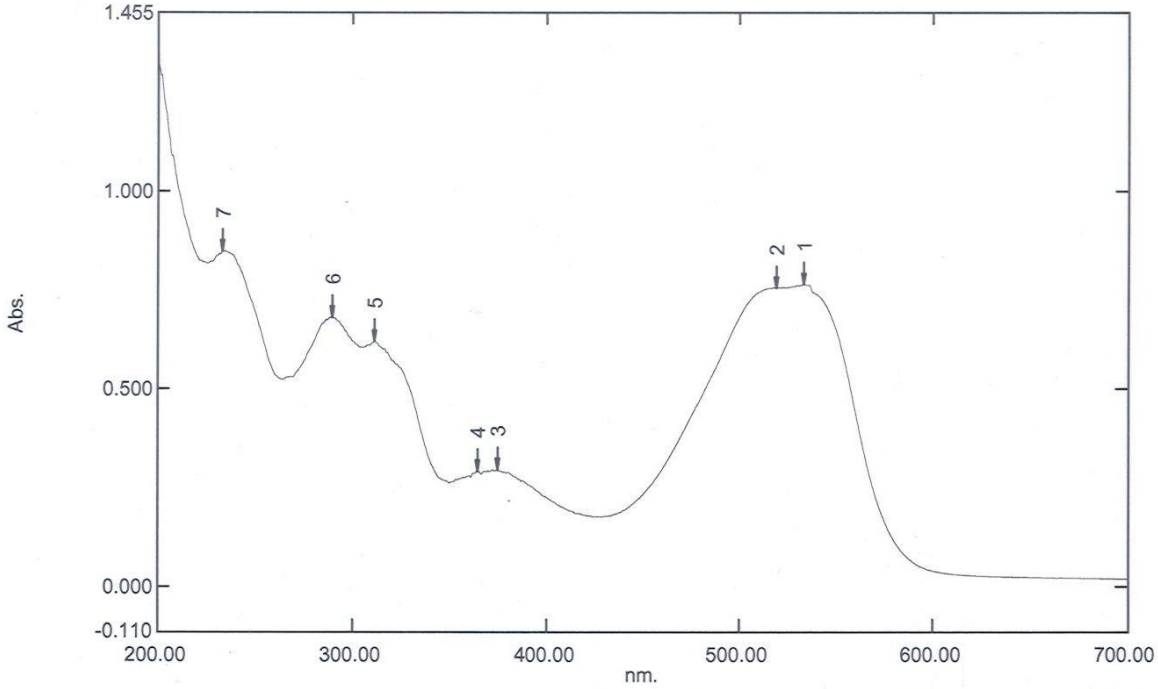

Fig 4.3: UV- Vis spectrum of Reactive red 111 before decolorization. X-axis; represents the wavelength (nm). Y-axis; represents the Absorbance.

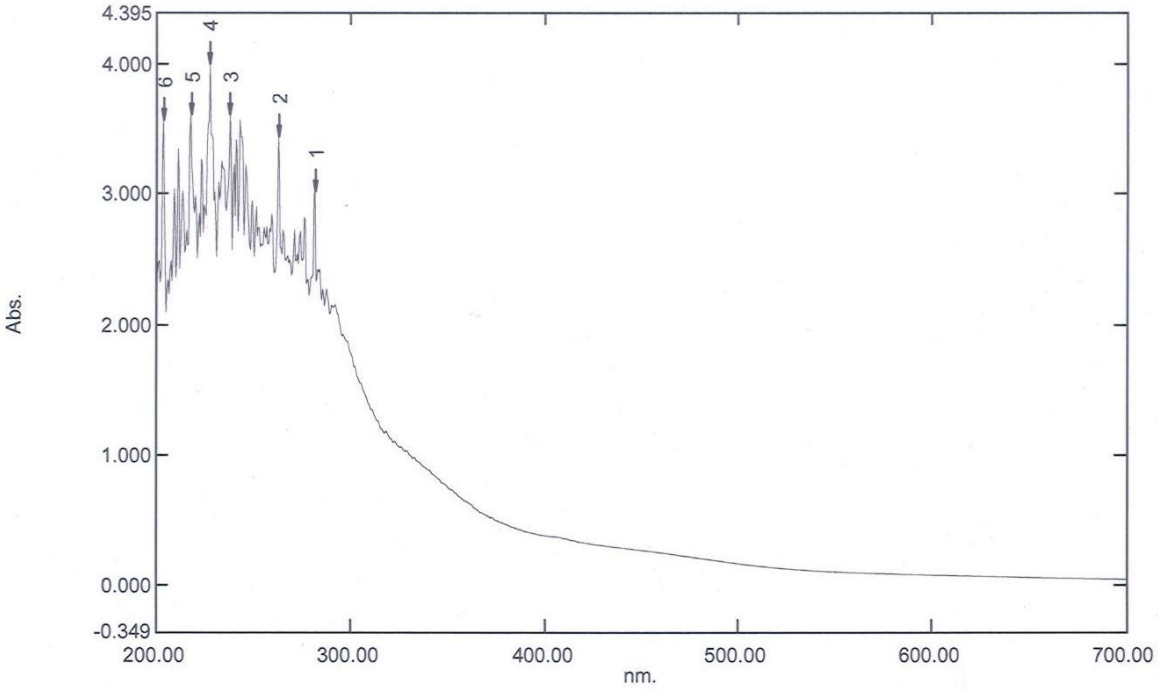

Fig 4.4: UV- Vis spectrum of Reactive red 111 after decolorization. X-axis; represents the wavelength (nm). Y-axis; represents the Absorbance.

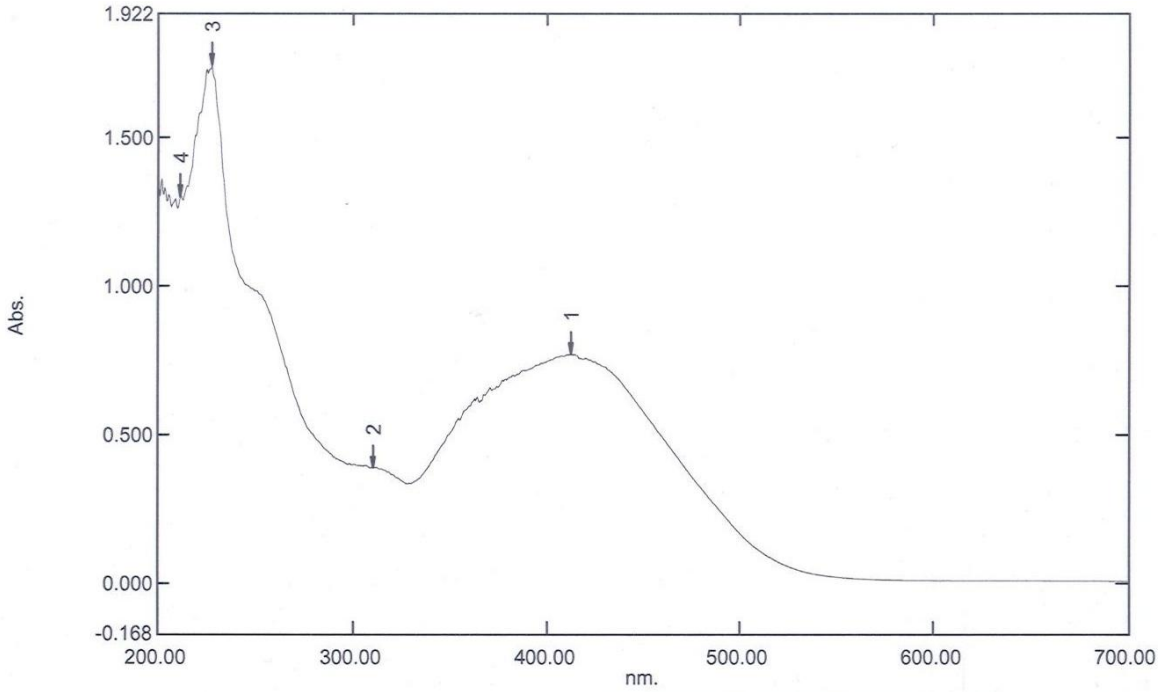

Fig 4.5: UV- Vis spectrum of Reactive yellow 44 before decolorization. X-axis; represents the wavelength (nm). Y-axis; represents the Absorbance.

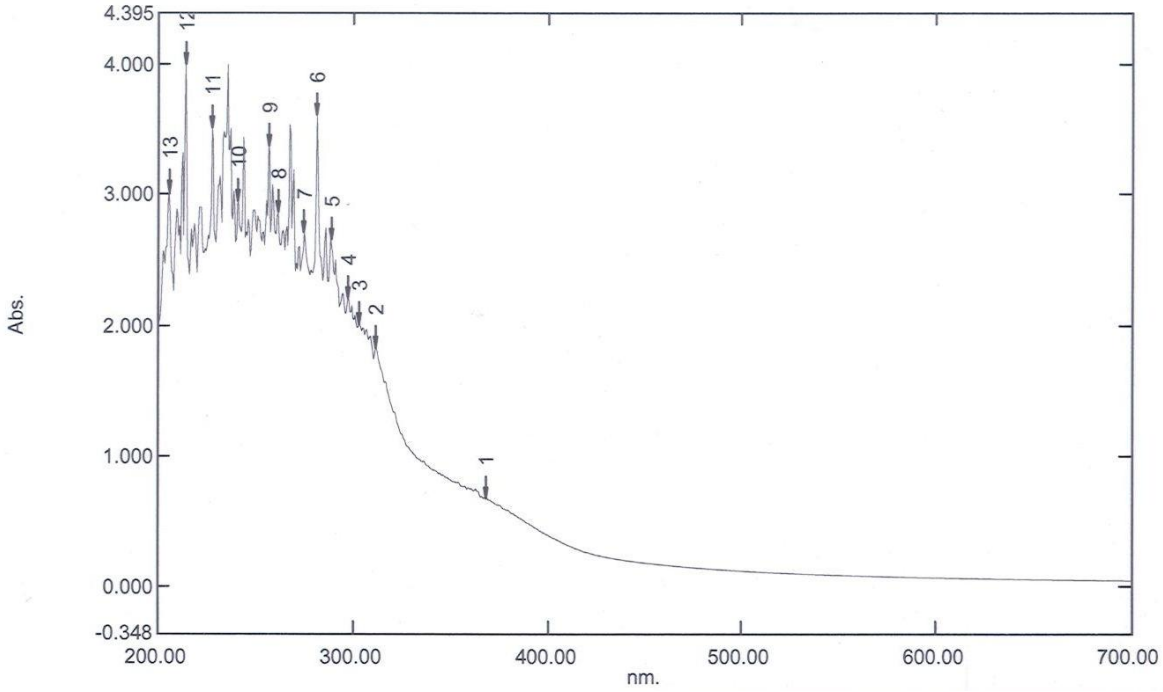

Fig 4.6: UV- Vis spectrum of Reactive yellow 44 after decolorization. X-axis; represents the wavelength (nm). Y-axis; represents the Absorbance.

4.5.2 FTIR analysis

The results of FTIR analysis of the untreated dye (control) and treated dye (sample) showed various peaks. Comparison of the FTIR spectrum of the untreated dyes with treated dyes clearly indicated biodegradation of the parent dyes by AMETH72. Untreated RB81 dye (control) Fig 4.7 showed peak at 1103 cm^{-1} for C-C bending vibration, peaks at 1485 cm^{-1} and 1558 cm^{-1} for aromatic ring vibration and C=C stretching in benzene ring respectively. An overtone band near 1260 cm^{-1} indicated aromatic nature of the dye. The peak at 1404 cm^{-1} for -N=N- stretch and peaks at 1118 cm^{-1} and 1242 cm^{-1} for –C-N stretch confirmed the azo nature of the dye. Peaks at 1169 cm^{-1}, 1633 cm^{-1}, 2092 cm^{-1} and 3412 cm^{-1} represented –C-N stretch of aromatic nitro-compounds, -OH stretching, C≡C stretching and N-H stretching respectively. Peaks at 1331 cm^{-1} for S-O stretching vibration and 1350 cm^{-1} for S=O stretching vibrations indicated the sulfonic nature of the dye. The FTIR spectra of treated RB81 dye (Fig 4.8) displayed peaks at 1639 cm^{-1} for N-H bend, peak at 2372 cm^{-1} for C=N vibration, peak at 2092 cm^{-1} for C≡C stretching of alkynes and peaks at 1161 cm^{-1}, 3387 cm^{-1} for N-H stretching of amines. However, peak at 1500 cm^{-1} indicated conversion of amines to nitroalkanes. The peak at 1629 cm^{-1} indicated NO_2 vibrations of nitrates. The peaks at 1076 cm^{-1}, 1321 cm^{-1} for S-O stretching and peak at 1095 cm^{-1} for S=O stretching suggested the formation of sulfonic acids and sulfoxides.

For the untreated RR111 dye, the FTIR spectra (Fig 4.9) showed peak at 3114 cm^{-1} for C-H stretching of aromatic compounds and a peak at 751 cm^{-1} confirmed the aromatic nature of the dye. The peak at 1614 cm^{-1} for -N=N- stretching indicated the azo nature of the dye. The untreated RR111 also showed peak at 2080 cm^{-1} for C≡C stretching, a peak at 2357 cm^{-1} for C≡N stretching, a peak at 3221 cm^{-1} for –OH stretch and peaks at 3305 cm^{-1}, 3325 cm^{-1}, 3372 cm^{-1} for N-H stretching vibrations. The FTIR spectra of treated RR111 dye (Fig 4.10) revealed peak at 767 cm^{-1} for C-H stretching due to deformation of benzene, a peak at 3245 cm^{-1} for -OH stretching, a peak at 3061 cm^{-1} for C-H stretching of aromatic homocyclic compounds and a peaks at 3308 cm^{-1} and 3362 cm^{-1} for N-H stretching vibrations. The peak at 2037 cm^{-1} indicated the formation of imines.

The FTIR analysis of the untreated RY44 dye (Fig 4.11) showed peak at 2924 cm^{-1} for asymmetric $–CH_3$ stretching vibration, a peak at 3244 cm^{-1} for -OH stretch, a peak at 3384 cm^{-1} for N-H stretching vibration and a peak at 2851 cm^{-1} for O-H stretching vibration of quinone oximes. The peak at 1616 cm^{-1} for -N=N- stretching confirmed the azo nature of the dye. For the treated RY44 dye the FTIR spectra (Fig 4.12) displayed peak at 1205 cm^{-1} for C-H deformation vibrations, peaks at 676 cm^{-1}, 733 cm^{-1}, 766 cm^{-1}, 847 cm^{-1} for loss of benzene ring, a peak at 1648 cm^{-1} for NO_2 asymmetric stretching of nitrates, a peak at 1654 cm^{-1} for N=O stretch of nitrite, peak at 3230 cm^{-1} for -OH stretch and peak at 3409 cm^{-1} for N-H stretching. The peaks at 2084 cm^{-1} and 2360 cm^{-1} represented C≡C stretching of alkynes and C≡N stretching vibrations respectively. The peak at 3432 cm^{-1} corresponds for free $-NH_2$ asymmetric stretching vibrations. The peak at 3061 cm^{-1} was due to C-H stretching of aromatic homocyclic compounds. The peak at 1663 cm^{-1} indicated the formation of oximes. (Jeffery et al., 1989; Stuart, 2004).

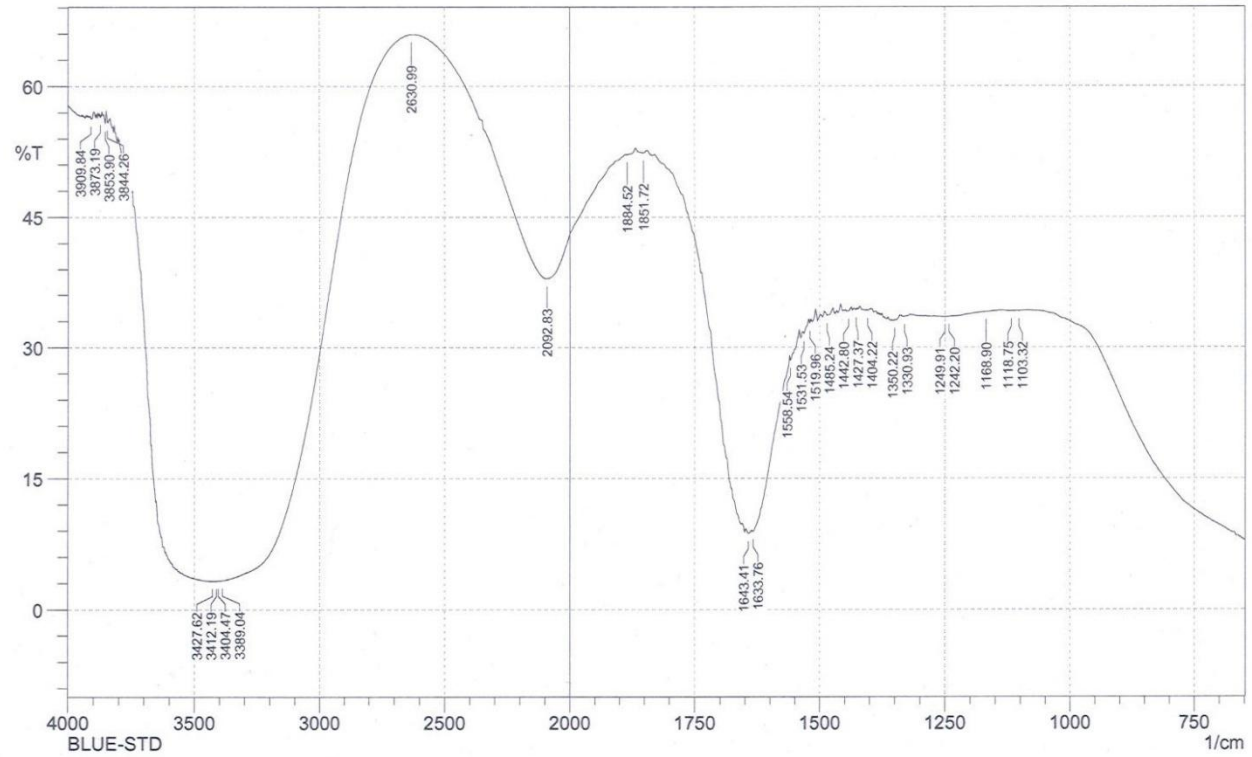

Fig 4.7: FTIR spectrum of Reactive blue 81 before degradation. X-axis; represents the Wave-number (cm^{-1}). Y-axis; represents the % Transmittance.

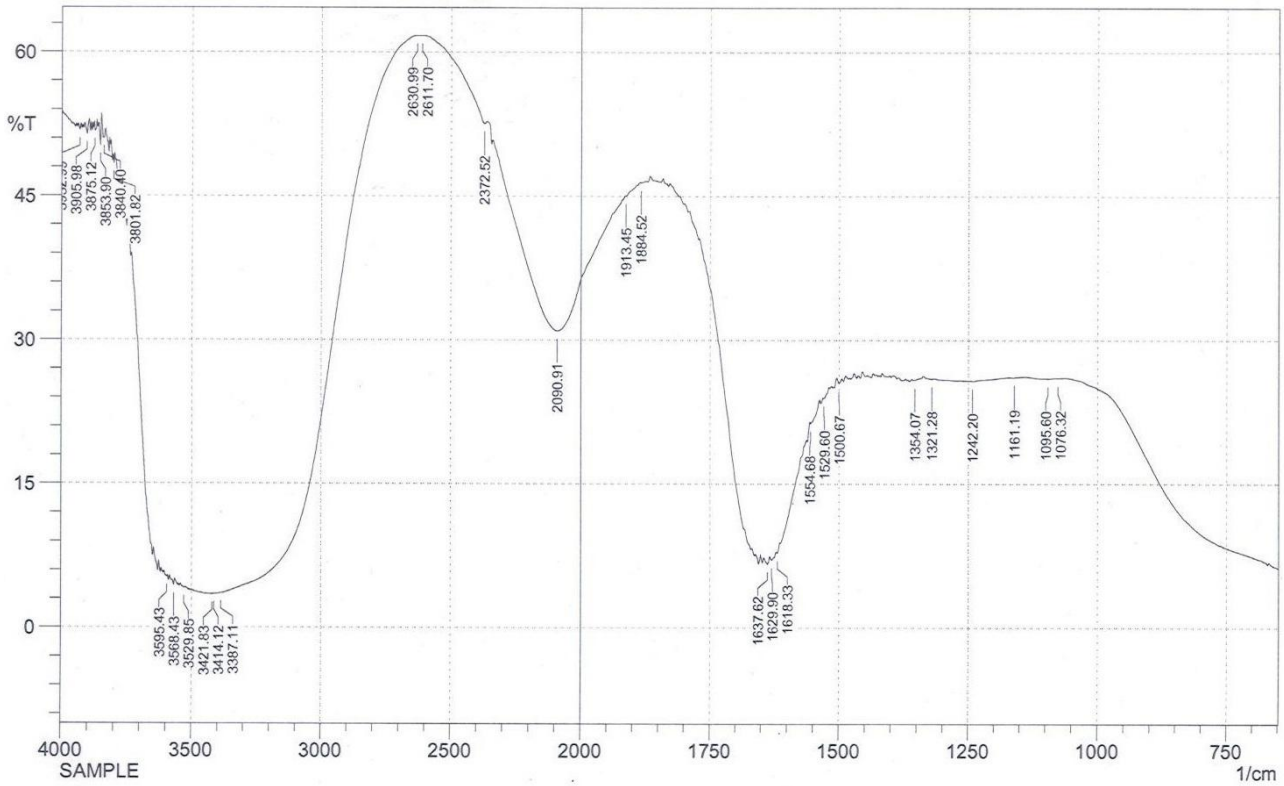

Fig 4.8: FTIR spectrum of Reactive blue 81 after degradation. X-axis; represents the Wave-number (cm^{-1}). Y-axis; represents the % Transmittance.

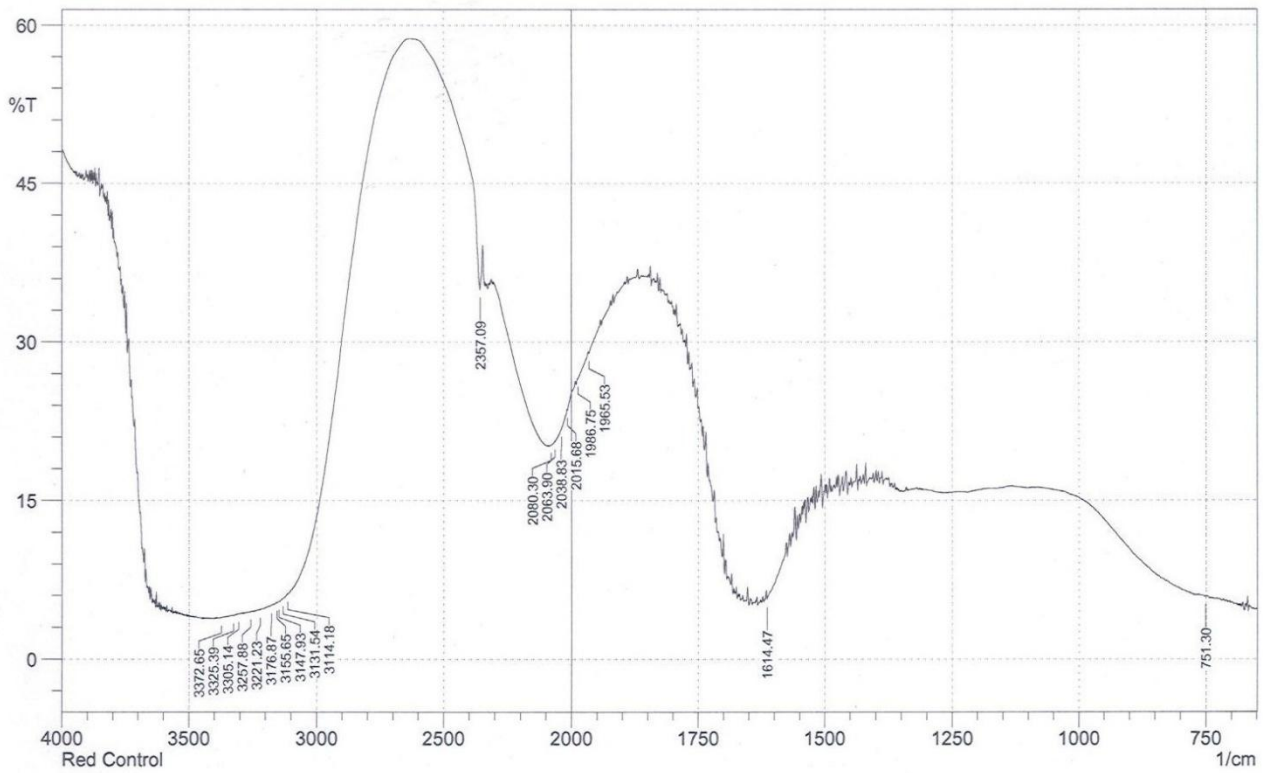

Fig 4.9: FTIR spectrum of Reactive red 111 before degradation. X-axis; represents the Wave-number (cm^{-1}). Y-axis; represents the % Transmittance.

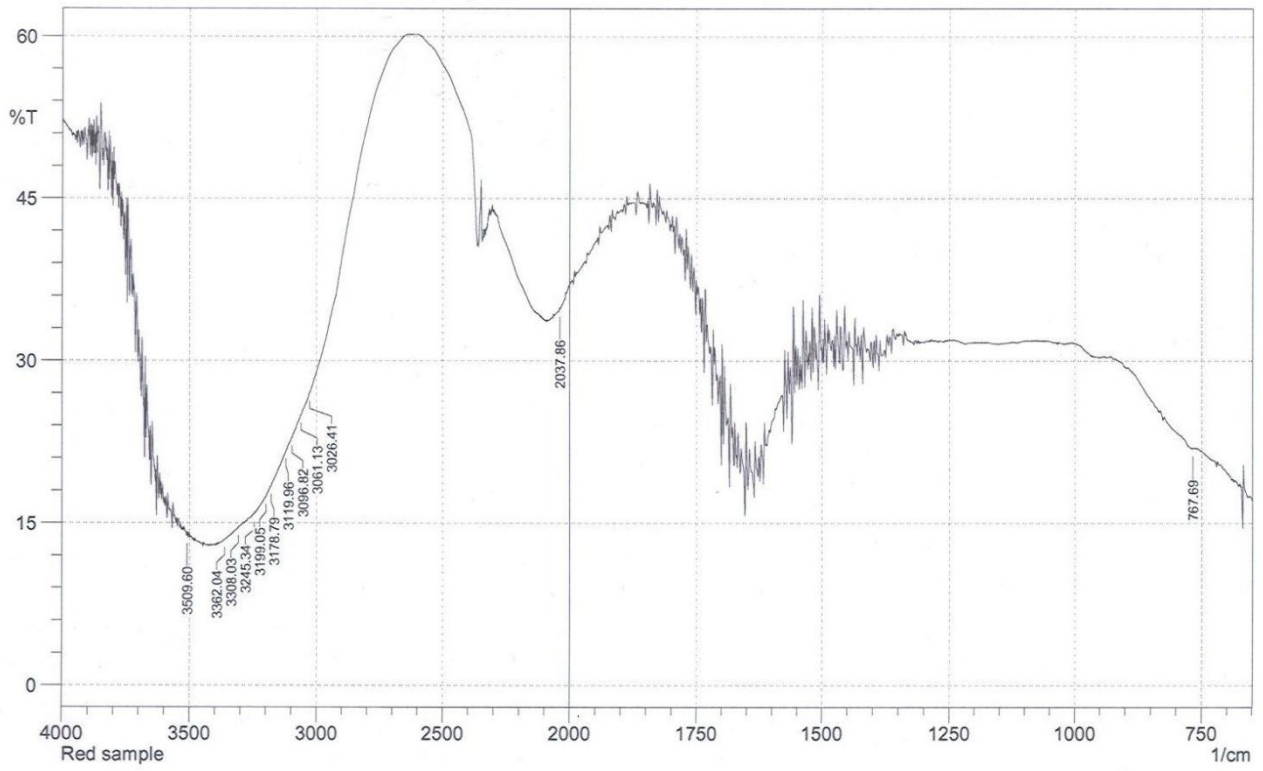

Fig 4.10: FTIR spectrum of Reactive red 111 after degradation. X-axis; represents the Wave-number (cm^{-1}). Y-axis; represents the % Transmittance.

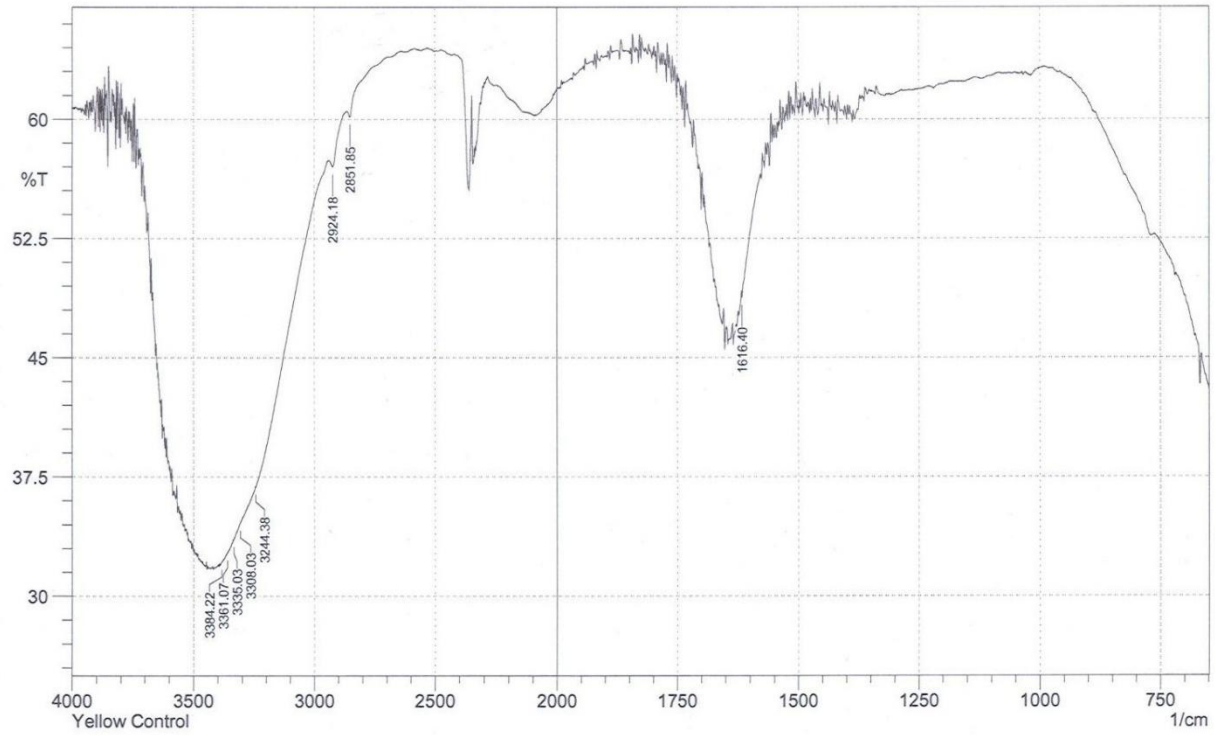

Fig 4.11: FTIR spectrum of Reactive yellow 44 before degradation. X-axis; represents the Wave-number (cm^{-1}). Y-axis; represents the % Transmittance.

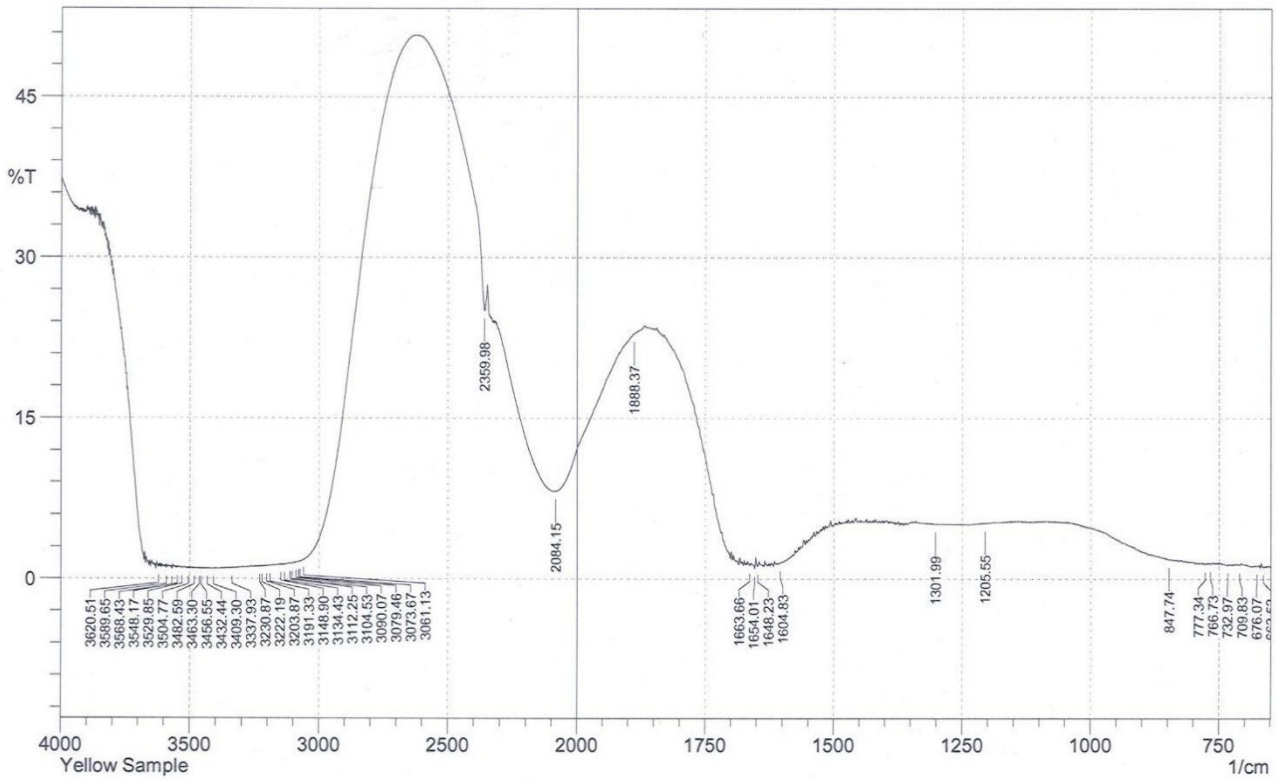

Fig 4.12: FTIR spectrum of Reactive yellow 44 after degradation. X-axis; represents the Wave-number (cm^{-1}). Y-axis; represents the % Transmittance.

4.6 Evaluation of bioremediation potential of the efficient bacterial strain

4.6.1 Seed germination study (Plate assay)

The effect of untreated dyes and treated dyes on the germination of wheat and Green gram is shown in Fig 4.13 and Fig 4.14 respectively. Both the wheat and Green gram showed good germination in the presence of treated dyes as compared to untreated dyes. For instance, the treated RR111 dye in wheat seeds showed 60% germination while the untreated RR111 dye showed only 20% germination.

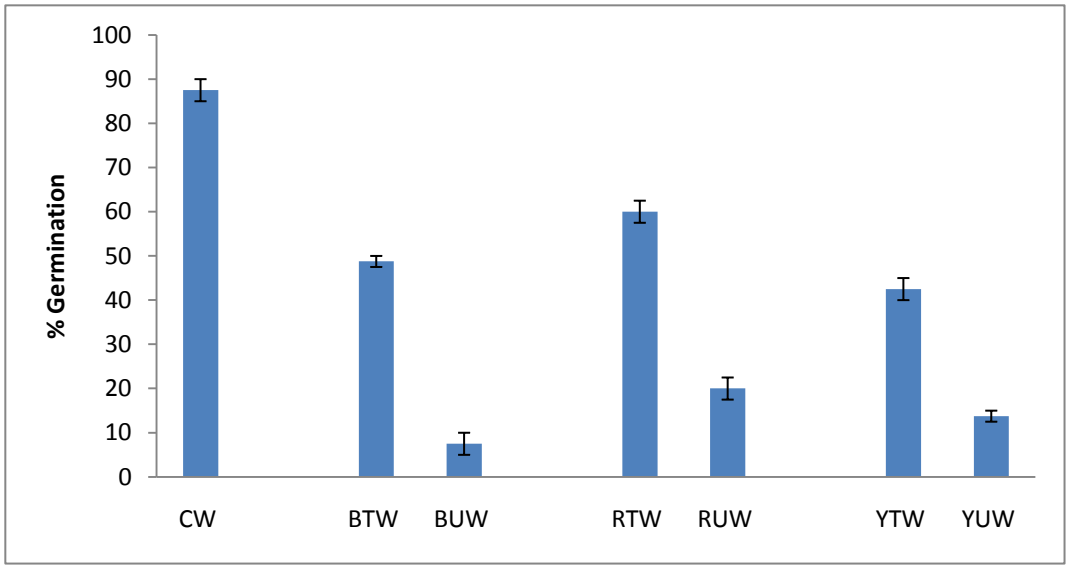

Fig 4.13: Effect of untreated and treated dyes on the seed germination of wheat.

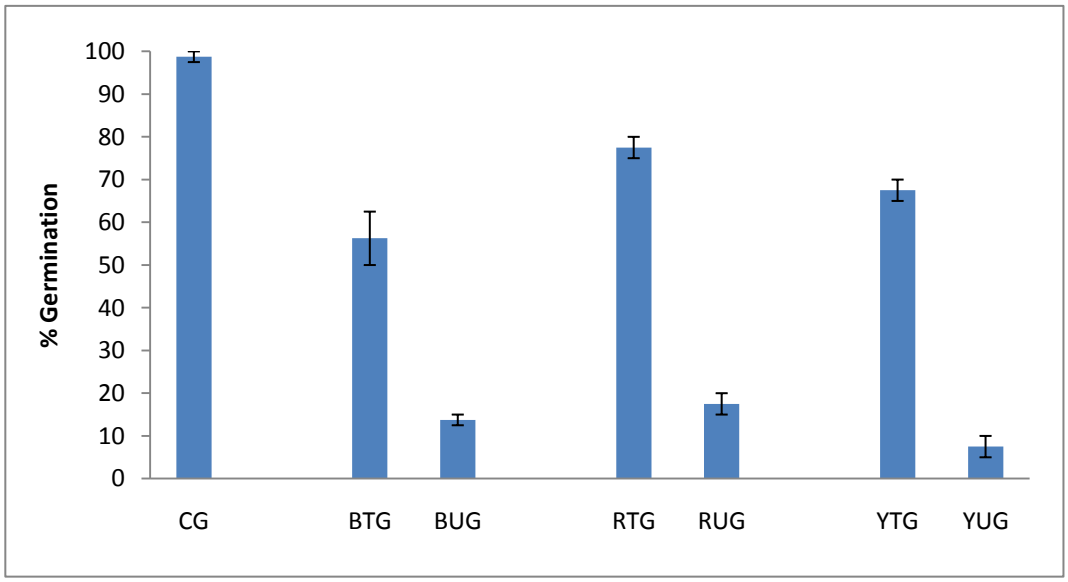

Fig 4.14: Effect of untreated and treated dyes on the seed germination of Green gram.

4.6.2 Seedling growth study (Pot assay)

The seedling growth for both the plants (Fig 4.15, Fig 4.16) was good in the presence of treated dyes as compared to the untreated dyes. In fact, the seedling growth in the presence of treated dyes was almost equivalent to that of the control which was grown in the presence of distilled water. However, the seedling growth of Green gram in the presence of treated and untreated RB81 and RY44 dyes were almost the same.

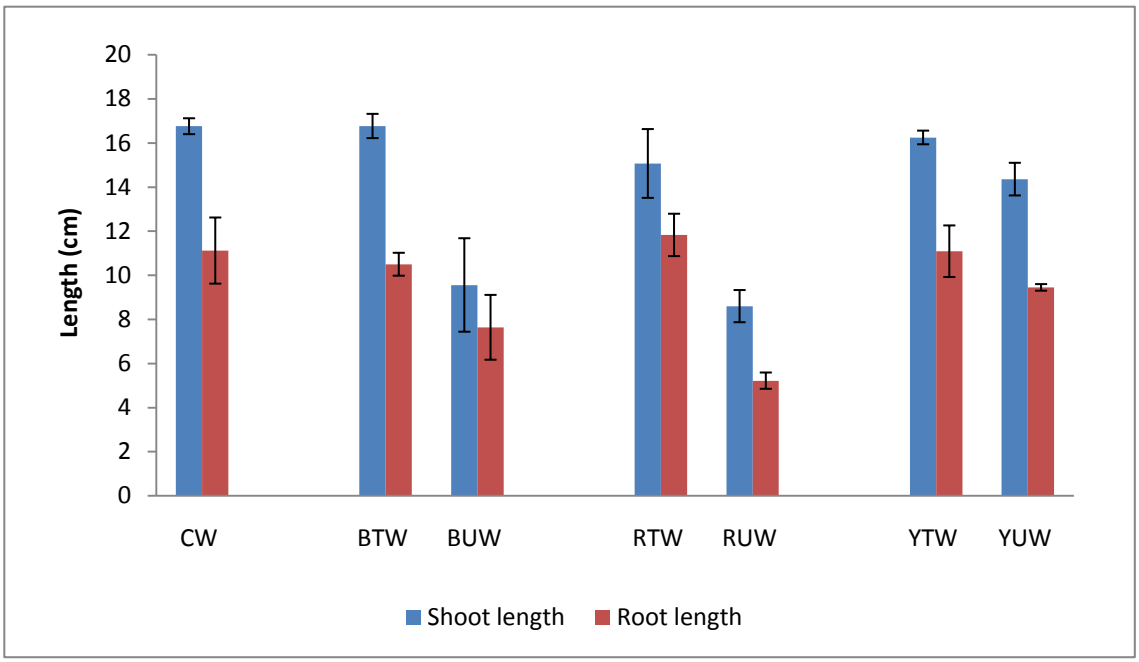

Fig 4.15: Effect of untreated and treated dyes on the growth of wheat seedling.

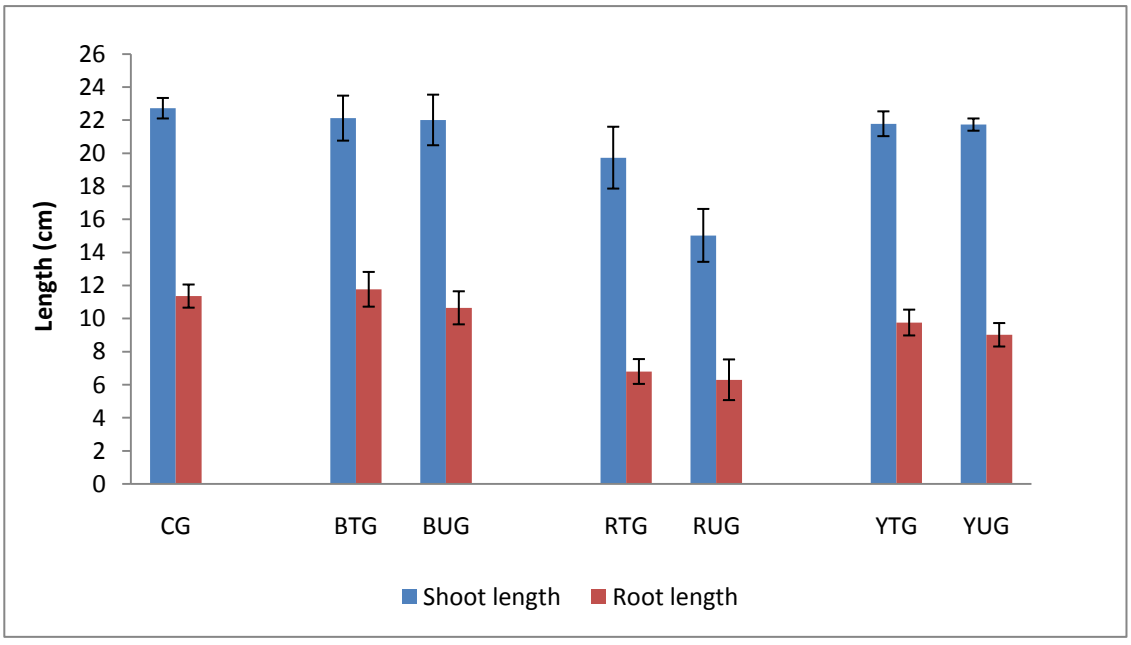

Fig 4.16: Effect of untreated and treated dyes on the growth of Green gram seedling.

4.6.3 Effect of degraded dye on physiochemical parameters of crop plant seedlings

4.6.3.1 Estimation of total carbohydrates and protein content of the crop plant seedlings

The carbohydrate and protein content in both the plants (Fig 4.17, Fig 4.18) were significantly higher in the presence of treated dyes than in the untreated dyes. In almost all the treated dyes (for both the plants) the carbohydrates and protein content was higher than the control.

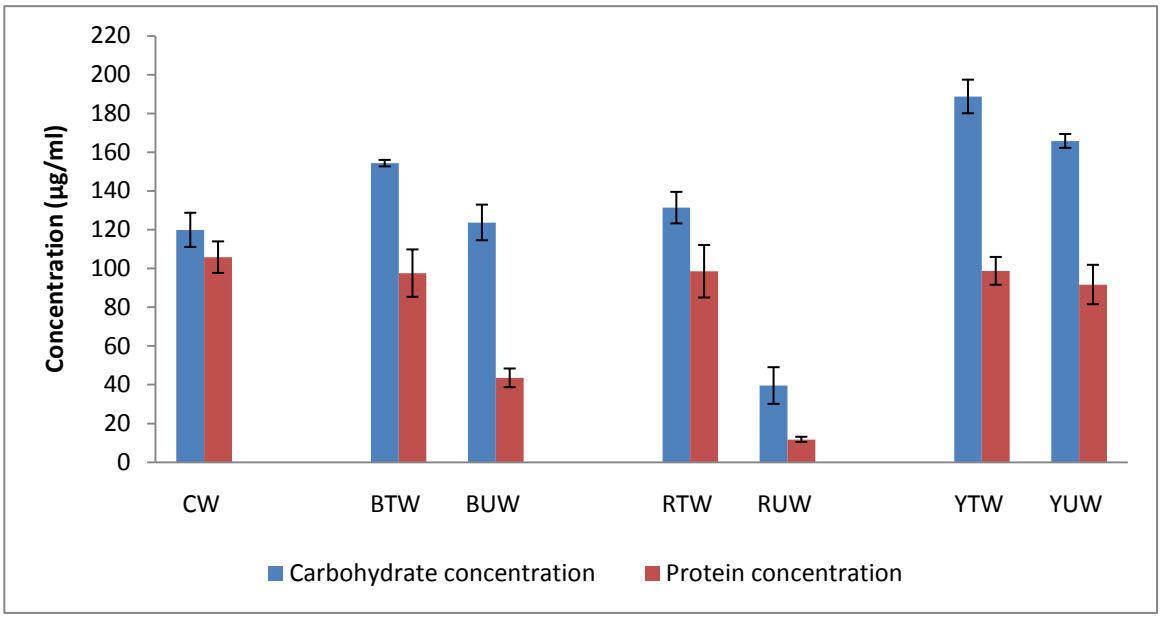

Fig 4.17: Effect of untreated and treated dyes on total carbohydrate and protein content of wheat seedlings.

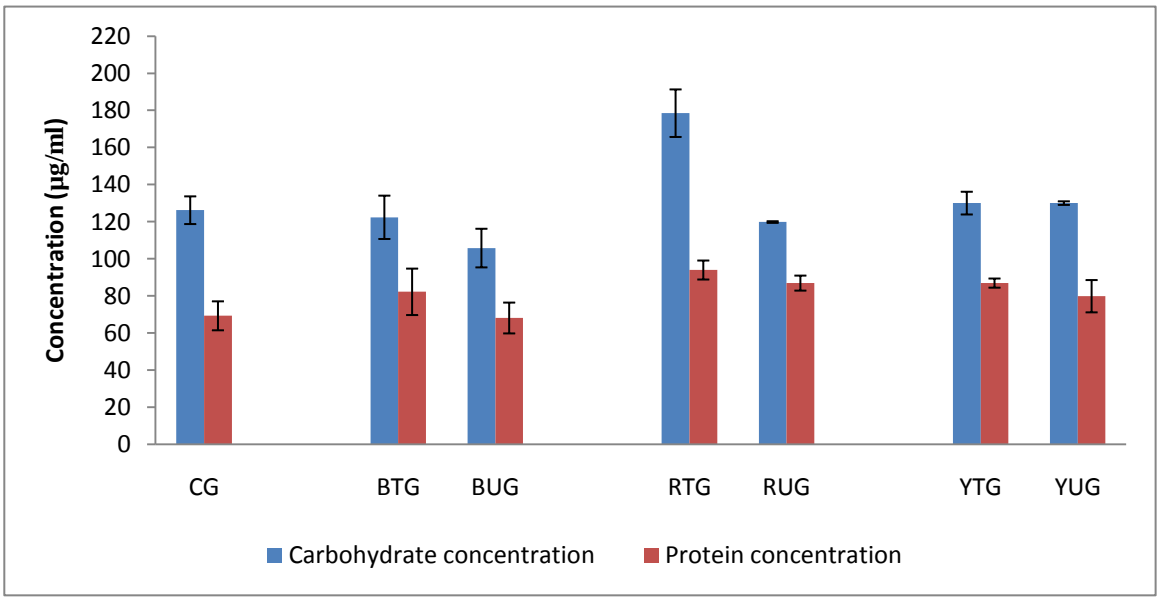

Fig 4.18: Effect of untreated and treated dyes on total carbohydrate and protein content of Green gram seedlings.

4.6.3.2 Estimation of total chlorophyll content of crop plant seedlings

The effect of untreated and treated dyes on the total chlorophyll content in wheat and Green gram plants are shown in Fig 4.19 and Fig 4.20 respectively. As expected the total chlorophyll content in both the plants were higher in the presence of treated dyes than in the presence of untreated dyes. The Green gram grown in treated dyes had chlorophyll content higher than that of the control.

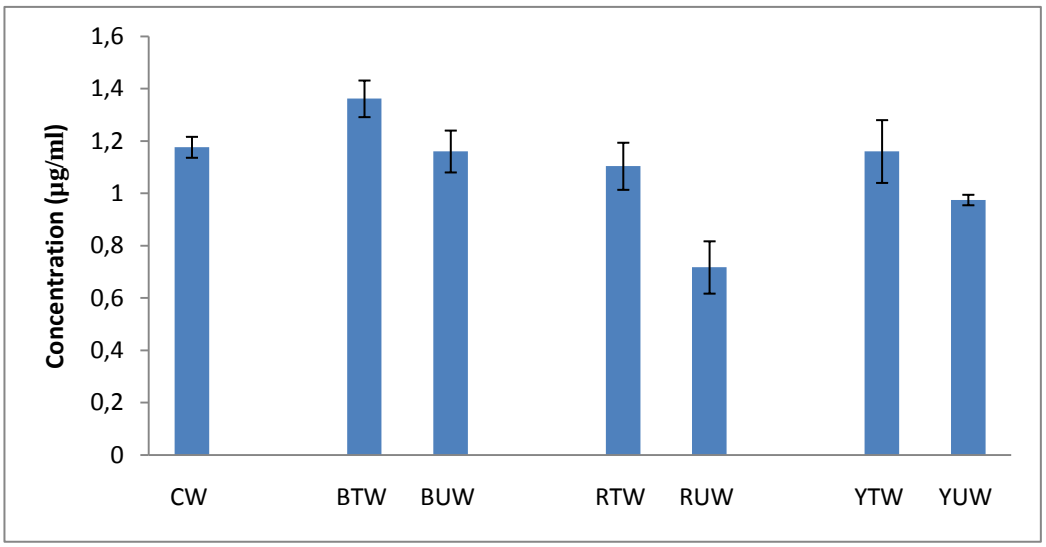

Fig 4.19: Effect of untreated and treated dyes on total chlorophyll content of wheat seedlings.

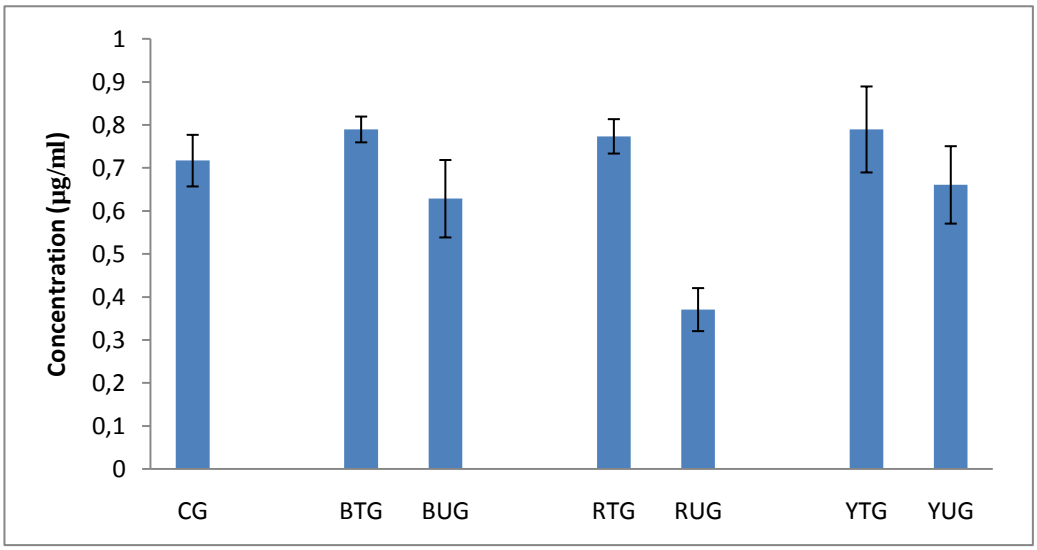

Fig 4.20: Effect of untreated and treated dyes on total chlorophyll content of Green gram seedlings.

4.7 Identification of efficient bacterial strain AMETH72

The AMETH72 bacterial strain is Gram-negative, rod shaped and motile. It is a non-sporulating and oxidase- and catalase- positive. The 1456 bp of 16S rDNA gene of AMETH72 strain was determined. The nucleotide alignment of the strain supported bootstrap values of 99% phylogenetic similarity to *Halomonas elongata.* The evolutionary distance was based on Kimura-2-parameter model (Kimura, 1980). *Escherichia coli* was used as the outgroup. The phylogenetic tree of the isolate AMETH72 is shown in Fig 4.21.

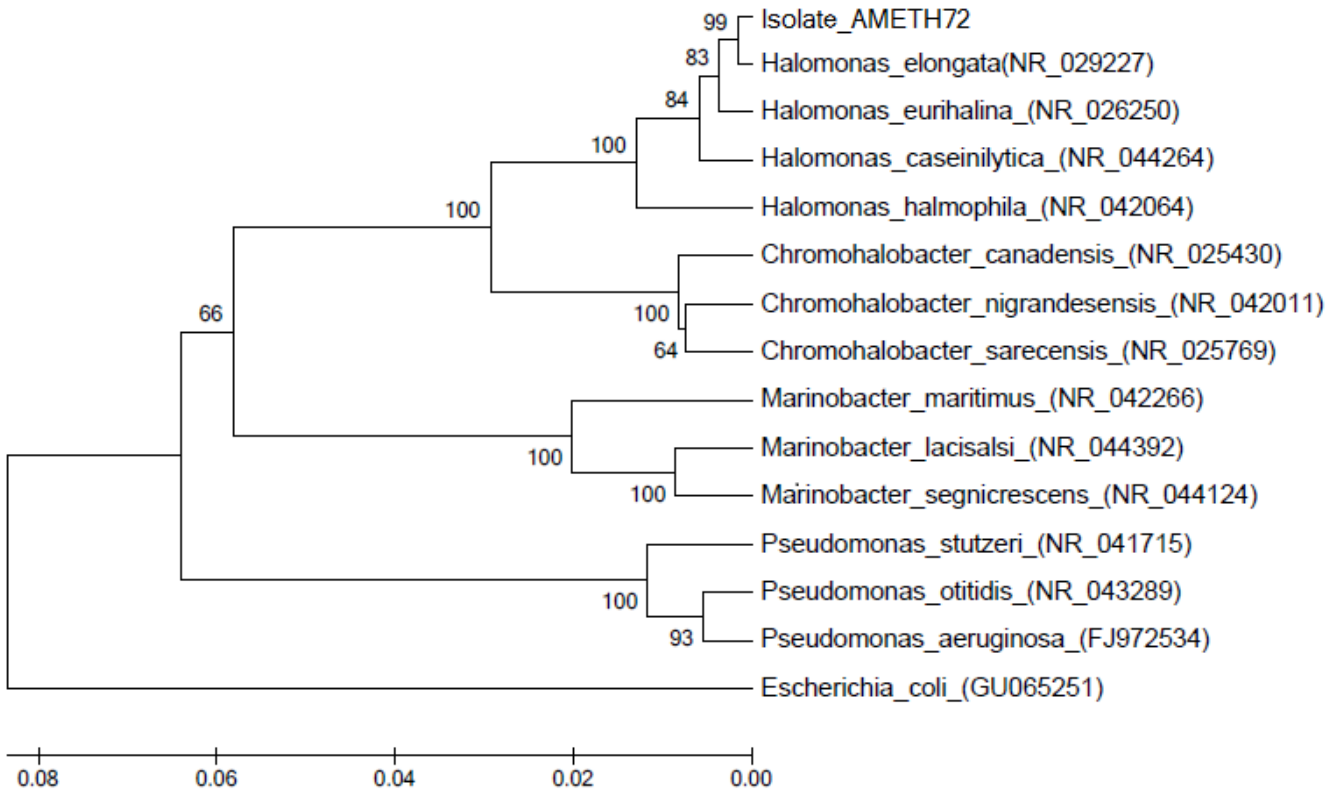

Fig 4.21: Phylogenetic tree of isolate AMETH72 drawn using Neighbour joining method by Kimura-2-parameter with 1000 replicates in MEGA 5.

5 DISCUSSION

The present work focuses on the use of halotolerant microorganism to remediate the environment contaminated by azo dyes, which are extensively used in the textile industries. The presence of high salt content in the textile dye effluents hinders the development of efficient bio-treatment system to bioremediate the textile azo dyes. This imposes a great need in developing bacterial strains that could thrive under high salt conditions. Salterns or Solar salt crystallizer ponds contain hyper-saline waters and the soil present there serves as a rich

source of marine microorganisms. The bacteria isolated from such saline soil will definitely yield a good collection of halophilic and halotolerant bacterial strains.

Halotolerant bacteria has been reported to decolorize textile azo dyes (Khalid et al., 2008). The azo dyes are degraded by bacteria using their extracellular hydrolytic and oxidative enzymes (Axelsson et al., 2006; Wang et al., 2009). In this work, the bacteria isolated from the Kelambakkam solar salt crystallizer ponds were first screened for their ability to produce tannase and laccase enzymes. The presence of tannase was detected by using tannic acid as an indicator compound. The tannase producing bacterial strains showed dark-brown zone formation on the agar medium containing tannic acid. The oxidation of tannic acid by tannase enzyme resulted in the formation of gallic acid that caused brown coloration (Katwa et al., 1981). It catalyses the hydrolysis of esters and depside bonds present in the hydrolysable tannins or gallic acid esters producing glucose and gallic acid. Screening of laccase producing bacteria was done on medium containing the indicator compound guaiacol. In the presence of guaiacol an intense reddish brown color observed in the medium around the bacterial colonies was taken as a positive reaction for laccase enzyme activity as previously reported (Ang et al., 2011; Collins and Dobson, 1997; Kiiskinen et al., 2004; Kumar et al., 2011; Viswanath et al., 2008). Chivukula and Renganathan (1995) reported the role of laccase in azo dye degradation. Their study suggested that laccase oxidation resulted in detoxification of the azo dyes.

Decolorization of the azo dyes takes place either by adsorption or biodegradation by the bacteria (Aravindhan et al., 2007; Knapp and Newby, 1995; Kumar et al., 2007). In the case of adsorption the cell pellets are colored whereas cell pellets retaining their original color shows the occurrence of biodegradation (Chen et al., 2003). The cell pellets of all the 11 selected bacterial strains, after decolorization of RB81, RR111 and RY44 retained their original color. This indicated that the decolorization occurred due to biodegradation and not by adsorption. The decolorization percentage remarkably increased after the strains- AMETH72 and AMETH77 were immobilised. The decolorization percentage was higher when the cells were immobilized and lower when the cells were free. This might suggest that by immobilization, the toxic effect of the recalcitrant dyes on the growth rate of the bacteria was nullified. It might also be attributed to the increase in microbial activity inside the immobilized beads or creation of low- oxygen microenvironment due to diffusion resistance (He et al., 2004). Similarly, Su et al. (2009) reported accelerated azo dye decolorization by anthraquinone and quinine- reducing bacterial consortium through immobilization in calcium alginate. Chen and Lin (2007) used alginate-silicate immobilized *Pseudomonas luteola* for decolorizing azo dye- Reactive Red 22. The decolorization in Repeated- batch experiment was used to compare the two bacterial strains AMETH72 and AMETH77 and to select the most efficient strain. The immobilized AMETH72 showed higher decolorization than immobilized AMETH77 in Batch #1 (Appendix 2). For all the 3 azo dyes, the decolorization percentage reached the highest values in immobilized AMETH72. Therefore, AMETH72 was concluded to be the most efficient bacterial strain isolated in this work. The Repeated- batch experiment also showed the stability and potential of immobilized AMETH72 for repeated use in wastewater treatment systems.

In the UV- Vis spectral analysis, the absorbance signature of the azo dyes consisted a major peak in the visible region at 576 nm, 533 nm and 413 nm for RB81, RR111 and RY44 respectively (Fig 4.1, Fig 4.3 and Fig 4.5). If the dye removal is due to biodegradation, either the absorbance peak in the visible region completely disappear or a new peak will appear (Yu and Wen, 2005). After decolorization the major absorbance peaks disappeared completely, indicated complete cleavage of the chromophoric (-N=N-) group and also supported the earlier conclusion that the decolorization was due to biodegradation, rather than inactive surface adsorption. The UV spectra of the decolorized dye RB81 (Fig 4.2), showed absorbance peaks at 206 nm and 228 nm corresponding to methyl acetate and 1-buten-3-yne respectively. In decolorized RR111 (Fig 4.4), absorbance peak at 217 nm indicated the presence of 1,3 butadiene. The decolorized RY44 (Fig 4.6), showed peaks at 256 nm and 275 nm corresponding to 1,3 cyclohexadiene and 1,3,5- Hexatriene (Jeffery et al., 1989). Hence, the UV spectral analysis clearly indicated the presence of alkanes and alkenes in the decolorized culture and also confirmed that the dyes were broken-down to different products. The FTIR technique has been used previously by some workers for analyzing azo dye degraded products (Elisangela et al., 2009; Kalyani et al., 2008; Parshetti et al., 2010; Shedbalkar and Jadhav, 2011). In the FTIR analysis, peaks for the –N=N- disappeared completely from the spectrum of treated azo dyes which confirmed the previous UV- Vis analysis results relating to the azo linkage disruption. The aromatic amines are the primary products formed by the cleavage of azo linkages in the azo dyes. Kudlich et al. (1999) reported that many of the aromatic amines were sensitive to autoxidation leading to the formation of dimers and eventually to dark colored autoxidation products. However, in the present study no increase in the color of the decolorized dyes was observed. This indicated that the aromatic amines were biodegraded effectively. The FTIR analysis also confirmed the biodegradation of the azo dyes to different products like sulfoxides, sulfonic acids, nitrates, nitrites, alkanes, alkenes, imines and oximes.

The discharge of untreated azo dyes from the textile industries into the water bodies causes environmental and health hazards. Moreover, things get worse when the dye contaminated water reaches agricultural fields. Therefore it becomes important to account on the phyto-toxocity and crop plant growth in the presence of untreated and treated dyes. The plant growth promotion studies were conducted on the common crop plants in India- *Triticum aestivum* (wheat) and *Vigna radiata* (Green gram). The studies revealed high germination (%) and significant growth in shoots and roots of both the crop plants grown in treated dyes as compared to the untreated dyes. This confirmed the biodegradation of the dyes by AMETH72 , which resulted in detoxification and improvement of plant growth in the presence of treated dyes. Similar results were reported by Shedbalkar and Jadhav (2011), where *Triticum aestivum* and *Ervum lens* Linn seeds were tested for phytotoxicity towards malachite green and its degraded metabolites by *Penicillium ochrochloron*. In the present study, the total carbohydrates, total proteins and total chlorophyll content was also higher in both the crop plants growth in treated dyes as compared to the untreated dyes. This showed that the metabolites in the treated dye increased the sugar, protein and chlorophyll content in both the crop plants, while the untreated dyes reduced the concentration of sugars, proteins and chlorophyll in both the crop plants. However, it was observed in some cases that the total

carbohydrate/ protein/ chlorophyll content in untreated dyes were higher than that of the control. This might be due to the physiological stress responses induced by the toxic untreated azo dyes.

The 16S rRNA analysis revealed that the isolated strain AMETH72 is *Halomonas elongata*. It is a gram- negative bacterium isolated from the rhizosphere region of halophytes growing near the solar salt crystallizer ponds, Kelambakkam, India. The *Halomonas elongata* decolorized and degraded all the 3 azo dyes (RB81, RR111 and RY44) efficiently. However, there is no available literature on azo dye degradation by *Halomonas elongata.* Previous studies have shown that the strains of *Halomonas sp*. isolated from textile industries effluents were able to decolorize seven azo dyes- Remazol Black B, Remazol Black N, Sulfonyl Scarlet BNLE, Sulfonyl Blue TLE, Maxilon Blue and Entrazol Blue IBC. The strains were identified as *Halomonas aquamarina, Halomonas meridian, Halomonas salina* (Asad et al., 2007). Guo et al. (2008) isolated *Halomonas* strains from coastal sediments contaminated by chemical wastewater. They showed that under high salt concentration the isolated *Halomonas sp*. decolorized five azo dyes in 24 hours with a decolorization above 90%.

6 CONCLUSION

Dyes are designed to resist fading even against chemicals such as oxidizing agents. It is really amazing that these dyes stand no chance against microbial degradation. The bacterial strains isolated from Kelambakkam solar salt crystalliser ponds, were screened for the ability to produce extracellular tannase and laccase enzymes and for their ability to decolorize RB81, RR111 and RY44 azo dyes. The most efficient strain was chosen after the immobilization studies. The 16S rRNA sequencing of the most efficient bacterial strain AMETH72 showed 99% similarity to *Halomonas elongata*. The analysis of degradation products by FTIR and UV- Vis analysis revealed disruption of azo linkages and subsequent conversion of aromatic amines into simpler products. The treated dyes were found to improve plant growth and total chlorophyll content as compared to untreated dyes.

Bioremediation has proved to be very effective method in countering the textile dye pollution in an eco-friendly way. This approach creates a promising hope to remediate the environments polluted by textile azo dyes. Moreover, a lot of future work is needed to isolate new microorganisms capable of effectively degrading wide range of textile dyes and to create an environment free from textile dye pollution.

7 REFERENCES

Abadulla E, Robra KH, Gübitz GM, Silva LM, Cavaco-Paulo A. Enzymatic decolorization of textile dyeing effluents. Textile Research Journal (2000) 70:409-414.

Ang TN, Ngoh GC, Chua ASM. A quantitative method for fungal ligninolytic enzyme screening studies. Asia-Pacific Journal of Chemical Engineering (2011) 6:589-595.

Aravindhan R, Rao JR, Nair BU. Removal of basic yellow dye from aqueous solution by sorption on green alga Caulerpa scalpelliformis. Journal of Hazardous Materials (2007) 142:68-76.

Arnon DI. Copper Enzymes in Isolated Chloroplasts. Polyphenoloxidase in Beta Vulgaris (1949): Plant physiology. 1-15.

Arun Kumar RS, Rajesh Sawhney. Enzyme Mediated Amido Black Decolourization by Soil borne RS-II Strain Isolated from an Industrial Town. Nature and Science (2011) 9:125-131.

Asad S, Amoozegar MA, Pourbabaee AA, Sarbolouki MN, Dastgheib SMM. Decolorization of textile azo dyes by newly isolated halophilic and halotolerant bacteria. Bioresource Technology (2007) 98:2082-2088.

Axelsson J, Nilsson U, Terrazas E, Alvarez Aliaga T, Welander U. Decolorization of the textile dyes Reactive Red 2 and Reactive Blue 4 using Bjerkandera sp. Strain BOL 13 in a continuous rotating biological contactor reactor. Enzyme and Microbial Technology (2006) 39:32-37.

Babu KS, Ajith-Kumar PV, Kunhi AA. Simultaneous degradation of 3-chlorobenzoate and phenolic compounds by a defined mixed culture of Pseudomonas spp. World Journal of Microbiology and Biotechnology (1995) 11:148-152.

Balan DSL, Monteiro RTR. Decolorization of textile indigo dye by ligninolytic fungi. Journal of Biotechnology (2001) 89:141-145.

Banat IM, Nigam P, Singh D, Marchant R. Microbial decolorization of textile-dyecontaining effluents: A review. Bioresource Technology (1996) 58:217-227.

Chemblink. Reactive Blue 81. http://www.chemblink.com/products/75030-18-1.htm (accessed 3rd January, 2013) (English).

Chen JP, Lin YS. Decolorization of azo dye by immobilized Pseudomonas luteola entrapped in alginate-silicate sol-gel beads. Process Biochemistry (2007) 42:934-942.

Chen KC, Wu JY, Liou DJ, Hwang SCJ. Decolorization of the textile dyes by newly isolated bacterial strains. Journal of Biotechnology (2003) 101:57-68.

Chivukula M, Renganathan V. Phenolic azo dye oxidation by laccase from Pyricularia oryzae. Applied and Environmental Microbiology (1995) 61:4374-4377.

Collins PJ, Dobson ADW. Regulation of laccase gene transcription in Trametes versicolor. Applied and Environmental Microbiology (1997) 63:3444-3450.

Correia V, Stephenson T, Judd SJ. Characterisation of textile wastewaters - A review. Environmental Technology (1994) 15:917-929.

D. Mubarak Ali AS, R. Praveen Kumar, M. Gunasekaran, N. Thajuddin. Efficiency of Textile Dye Decolorization by Marine Cyanobacterium, Oscillatoria formosa NTDM02. African Journal of Basic & Applied Sciences (2011) 3:09-13.

Elisangela F, Andrea Z, Fabio DG, de Menezes Cristiano R, Regina DL, Artur CP. Biodegradation of textile azo dyes by a facultative Staphylococcus arlettae strain VN-11 using a sequential microaerophilic/aerobic process. International Biodeterioration and Biodegradation (2009) 63:280-288.

Faraco V, Pezzella C, Miele A, Giardina P, Sannia G. Bio-remediation of colored industrial wastewaters by the white-rot fungi Phanerochaete chrysosporium and Pleurotus ostreatus and their enzymes. Biodegradation (2009) 20:209-220.

Guo J, Zhou J, Wang D, Tian C, Wang P, Uddin MS. A novel moderately halophilic bacterium for decolorizing azo dye under high salt condition. Biodegradation (2008) 19:15-19.

He F, Hu W, Li Y. Biodegradation mechanisms and kinetics of azo dye 4BS by a microbial consortium. Chemosphere (2004) 57:293-301.

Jeffery GH, Bassett J, Mendham J, Denney RC. Vogel's Textbook of Quantitative Chemical Analysis. (1989) 5th edn. England: Longman Scientific and Technical.

Jin XC, Liu GQ, Xu ZH, Tao WY. Decolorization of a dye industry effluent by Aspergillus fumigatus XC6. Applied Microbiology and Biotechnology (2007) 74:239-243.

Kalyani DC, Patil PS, Jadhav JP, Govindwar SP. Biodegradation of reactive textile dye Red BLI by an isolated bacterium Pseudomonas sp. SUK1. Bioresource Technology (2008) 99:4635-4641.

Katwa LC, Ramakrishna M, Rao MRR. Spectrophotometric assay of immobilized tannase. Journal of Biosciences (1981) 3:135-142.

Khadijah.O LKK, Mohd Faiz F, Abdullah. Isolation, screening and development of local bacterial consortia with azo dyes decolourising capability. Malaysian Journal of Microbiology (2009) 5:25-32.

Khalid A, Arshad M, Crowley DE. Accelerated decolorization of structurally different azo dyes by newly isolated bacterial strains. Applied Microbiology and Biotechnology (2008) 78:361-369.

Kiiskinen LL, Rättö M, Kruus K. Screening for novel laccase-producing microbes. Journal of Applied Microbiology (2004) 97:640-646.

Kimura M. A simple method for estimating evolutionary rates of base substitutions through comparative studies of nucleotide sequences. Journal of Molecular Evolution (1980) 16:111-120.

Kirby N, Marchant R, McMullan G. Decolourisation of synthetic textile dyes by Phlebia tremellosa. FEMS Microbiology Letters (2000) 188:93-96.

Knapp JS, Newby PS. The microbiological decolorization of an industrial effluent containing a diazo-linked chromophore. Water Research (1995) 29:1807-1809.

Kudlich M, Hetheridge MJ, Knackmuss HJ, Stolz A. Autoxidation reactions of different aromatic o-aminohydroxynaphthalenes that are formed during the anaerobic reduction of sulfonated azo dyes. Environmental Science and Technology (1999) 33:896-901.

Kumar K, Devi SS, Krishnamurthi K, Dutta D, Chakrabarti T. Decolorisation and detoxification of Direct Blue-15 by a bacterial consortium. Bioresource Technology (2007) 98:3168-3171.

Kumar VV, Kirupha SD, Periyaraman P, Sivanesan S. Screening and induction of laccase activity in fungal species and its application in dye decolorization. African Journal of Microbiology Research (2011) 5:1261-1267.

Maier J, Kandelbauer A, Erlacher A, Cavaco-Paulo A, Gübitz GM. A New Alkali-Thermostable Azoreductase from Bacillus sp. Strain SF. Applied and Environmental Microbiology (2004) 70:837-844.

McMullan G, et al. Microbial decolourisation and degradation of textile dyes. Applied Microbiology and Biotechnology (2001) 56:81-87.

Mohandass Ramya, Bhaskar Anusha, S. Kalavathy, Devilaksmi S. Biodecolorization and biodegradation of Reactive Blue by Aspergillus sp. African Journal of Biotechnology (2007) 6:1441-1445.

Parshetti GK, Telke AA, Kalyani DC, Govindwar SP. Decolorization and detoxification of sulfonated azo dye methyl orange by Kocuria rosea MTCC 1532. Journal of Hazardous Materials (2010) 176:503-509.

Pierce J. Colour in textile effluents - the origins of the problem. Journal of the Society of Dyers & Colourists (1994) 110:pp 131-133.

Puvaneswari N, Muthukrishnan J, Gunasekaran P. Toxicity assessment and microbial degradation of azo dyes. Indian J Exp Biol (2006) 44:618-626.

Sadasivam S, Manickam A. Biochemical methods. (1996) 2nd edn. New Delhi: New Age International.

Saxena RM, Kewal PF, Yadav RS, Bhatnagar AK. Impact of tannery effluents on some pulse crops. Indian Journal of Environmental Health (1986) 28:345-348.

Senan RC, Abraham TE. Bioremediation of textile azo dyes by aerobic bacterial consortium. Biodegradation (2004) 15:275-280.

Shedbalkar U, Jadhav JP. Detoxification of malachite green and textile industrial effluent by Penicillium ochrochloron. Biotechnology and Bioprocess Engineering (2011) 16:196-204.

Shertate RS, Thorat P. Decolorization of Mordant Orange-1 by Marinobacter algicola MO-17. OnLine Journal of Biological Sciences (2012) 12:1-5.

Singh PP, Mall M, Singh J. Impact of fertilizer factory effluent on seed germination, seedling growth and chlorophyll content of gram (Cicer aeritenum). Journal of Environmental Biology (2006) 27:153-156.

Stuart BH. Infrared Spectroscopy: Fundamentals and Applications. (2004) 1st edn.: John Wiley & Sons. .

Su Y, Zhang Y, Wang J, Zhou J, Lu X, Lu H. Enhanced bio-decolorization of azo dyes by co-immobilized quinone-reducing consortium and anthraquinone. Bioresource Technology (2009) 100:2982-2987.

Viswanath B, Subhosh Chandra M, Pallavi H, Rajasekhar Reddy B. Screening and assessment of laccase producing fungi isolated from different environmental samples. African Journal of Biotechnology (2008) 7:1129-1133.

Wang H, Su JQ, Zheng XW, Tian Y, Xiong XJ, Zheng TL. Bacterial decolorization and degradation of the reactive dye Reactive Red 180 by Citrobacter sp. CK3. International Biodeterioration and Biodegradation (2009) 63:395-399.

Yu Z, Wen X. Screening and identification of yeasts for decolorizing synthetic dyes in industrial wastewater. International Biodeterioration and Biodegradation (2005) 56:109-114.

8 APPENDIX 1

Table 1: Composition of 3% Halophilic Agar medium.

Composition	**Amount**
Peptone	5 g
Yeast extract	3 g
Calcium chloride	0.1 g
Potassium chloride	5 g
Magnesium sulfate	6 g
Sodium chloride	30 g
Agar	20 g
Distilled water	1000 ml

Table 2:Phosphate buffer (0.1 M)

Components	**Amount**
Sodium dihydrogen phosphate	3.1 g
Disodium hydrogen phosphate	10.9 g
Distilled water	1000 ml

Table 3: Bradford reagent

Components	**Amount**
Coomassie Brilliant Blue G250	0.05% (w/v)
Ethanol	25 % (v/v)
Ortho- phosphoric acid	42.5 % (v/v)

The solution was made up to desired volume. When Coomassie brilliant blue G250 was completely dissolved, the solution was filtered with Whatman No.1 filter paper. The reagent was stored in amber bottle at 4^{o}C.

Table 4: Hugh and Leifon's OF basal medium

Composition	Amount
Peptone	2 g
Sodium chloride	5 g
Glucose	10 g
Bromthymol blue	0.03 g
Agar	3 g
Dipotassium phosphate	0.3 g
Distilled water	1000 ml

Table 5: Soil source of isolated bacterial strains.

Non- rhizosphere soil	Rhizosphere soil
AMETH 1- AMETH 8	AMETH9- AMETH 13
AMETH14- AMETH24	AMETH 25- AMETH 33
AMETH 34- AMETH 40	AMETH 41- AMETH 52
AMETH 53- AMETH 70	AMETH 71- AMETH 76
AMETH 77- AMETH 84	

Table 6: Colony morphology of isolated bacteria.

Sl. No.	Isolate code	Colony characteristics					
		Size	Colour	Shape	Margin	Elevation	Appearance
1	AMETH 1	Medium	Yellow	Circular	Entire	convex	Mucoid
2	AMETH 2	Large	Creamy white	Circular	Lobate	Flat	Semi-mucoid
3	AMETH 3	Medium	Orange	Circular	Entire	Umbonate	Mucoid
4	AMETH 4	Small	Powdery black	Circular	Entire	Raised	Dry
5	AMETH 5	Medium	Yellow	Circular	undulated	Umbonate	Mucoid
6	AMETH 6	Large	Pale red	Circular	Entire	Flat	Mucoid

7	AMETH 7	Large	White	Irregular	Lobate	Flat	Mucoid
8	AMETH 8	Large	Pale red	Circular	Entire	umbonate	Mucoid
9	AMETH 9	Medium	White	Circular	Entire	Flat	Semi-mucoid
10	AMETH 10	Medium	Yellow	Circular	Entire	convex	Mucoid
11	AMETH 11	Medium	Pale yellow	Circular	Entire	Umbonate	Mucoid
12	AMETH 12	Medium	White	Circular	Entire	Flat	Semi-mucoid
13	AMETH 13	Small	Pale red	Circular	Entire	Umbonate	Semi-mucoid
14	AMETH 14	Medium	Pale yellow	Irregular	Entire	Flat	Semi-mucoid
15	AMETH 15	Medium	Light pink	Circular	Entire	Umbonate	Mucoid
16	AMETH 16	Small	White	Circular	Entire	umbonate	Mucoid
17	AMETH 17	Small	Yellow	Circular	Entire	convex	Mucoid
18	AMETH 18	Small	Yellow	Circular	Entire	convex	Mucoid
19	AMETH 19	Small	Yellow	Circular	Entire	convex	Mucoid
20	AMETH 20	Large	White	Irregular	Lobate	Flat	Dry
21	AMETH 21	Small	Pale yellow	Circular	Entire	Umbonate	Semi-mucoid
22	AMETH 22	Large	White	Circular	undulated	Flat	Semi-mucoid
23	AMETH 23	Medium	White	Irregular	Entire	Flat	Semi-mucoid
24	AMETH 24	Small	Translucent white	Circular	Entire	Flat	Semi-mucoid
25	AMETH 25	Small	Pale red	Circular	Entire	convex	Mucoid
26	AMETH 26	Small	White	Circular	Entire	convex	Mucoid
27	AMETH 27	Small	White	Irregular	Entire	Flat	Mucoid
28	AMETH 28	Small	Red	Circular	Entire	Umbonate	Dry
29	AMETH 29	Small	Powdery black	Circular	Entire	Raised	Dry
30	AMETH 30	Small	White	Irregular	Entire	convex	Mucoid
31	AMETH 31	Small	White	Circular	Entire	convex	Mucoid
32	AMETH 32	Small	White	Circular	Entire	convex	Mucoid

33	AMETH 33	Small	White	Irregular	Entire	convex	Mucoid
34	AMETH 34	Small	white	Circular	Entire	convex	Mucoid
35	AMETH 35	Small	white	Circular	Entire	convex	Mucoid
36	AMETH 36	Small	white	Circular	Entire	convex	Mucoid
37	AMETH 37	Small	Powdery black	Circular	Entire	Raised	Dry
38	AMETH 38	Small	white	Circular	Entire	convex	Semi-mucoid
39	AMETH 39	Small	White	Circular	Entire	convex	Semi-mucoid
40	AMETH 40	Small	White	Circular	Entire	Umbonate	Dry
41	AMETH 41	Small	White	Circular	Entire	Convex	Mucoid
42	AMETH 42	Small	White	Circular	Entire	Convex	Mucoid
43	AMETH 43	Small	White	Circular	Entire	Convex	Mucoid
44	AMETH 44	Small	White	Circular	Entire	Convex	Mucoid
45	AMETH 45	Small	White	Irregular	Entire	Convex	Mucoid
46	AMETH 46	Small	White	Circular	Entire	Convex	Mucoid
47	AMETH 47	Small	White	Circular	Entire	Convex	Mucoid
48	AMETH 48	Small	Orange	Circular	Entire	Convex	Mucoid
49	AMETH 49	Small	Orange	Circular	Entire	Convex	Mucoid
50	AMETH 50	Small	Pale orange	Circular	Entire	Convex	Mucoid
51	AMETH 51	Medium	Translucent white	Circular	Entire	Convex	Mucoid
52	AMETH 52	Large	White	Circular	Serrate	Flat	Dry
53	AMETH 53	Large	Pale orange	Irregular	Entire	Convex	Mucoid
54	AMETH 54	Medium	White	Circular	Entire	Convex	Semi-mucoid
55	AMETH 55	Small	Pale orange	Irregular	Entire	Convex	Mucoid
56	AMETH 56	Small	White	Circular	Entire	Flat	Dry
57	AMETH 57	Small	Pale red	Circular	Entire	convex	Mucoid
58	AMETH 58	Small	Pale red	Circular	Entire	convex	Mucoid

59	AMETH 59	Tiny	White	Circular	Entire	convex	Mucoid
60	AMETH 60	Small	Translucent white	Circular	Entire	umbonate	Semi-mucoid
61	AMETH 61	Tiny	White	Circular	Entire	convex	Mucoid
62	AMETH 62	Tiny	White	Circular	Entire	convex	Mucoid
63	AMETH 63	Tiny	White	Circular	Entire	convex	Mucoid
64	AMETH 64	Tiny	Orange	Circular	Entire	umbonate	Semi-mucoid
65	AMETH 65	Small	Pale red	Circular	Entire	convex	Mucoid
66	AMETH 66	Small	Pale red	Circular	Entire	convex	Mucoid
67	AMETH 67	Small	Pale red	Circular	Entire	convex	Mucoid
68	AMETH 68	Small	White	Circular	Serrate	Flat	Dry
69	AMETH 69	Small	White	Circular	Entire	Umbonate	Semi-mucoid
70	AMETH 70	Small	White	Circular	Entire	convex	Mucoid
71	AMETH 71	Tiny	White	Circular	Entire	convex	Mucoid
72	AMETH 72	Tiny	White	Circular	Entire	convex	Mucoid
73	AMETH 73	Tiny	White	Circular	Entire	convex	Mucoid
74	AMETH 74	Tiny	White	Circular	Entire	convex	Mucoid
75	AMETH 75	Tiny	White	Circular	Entire	convex	Mucoid
76	AMETH 76	Tiny	White	Circular	Entire	convex	Mucoid
77	AMETH 77	Small	White	Circular	Entire	convex	Mucoid
78	AMETH 78	Small	White	Circular	Entire	convex	Mucoid
79	AMETH 79	Small	White	Circular	Entire	convex	Mucoid
80	AMETH 80	Small	White	Circular	Entire	convex	Mucoid
81	AMETH 81	Small	White	Circular	Entire	umbonate	Mucoid
82	AMETH 82	Small	White	Circular	Entire	convex	Mucoid
83	AMETH 83	Small	White	Circular	Entire	convex	Mucoid
84	AMETH 84	Small	White	Circular	Entire	convex	Mucoid

Table 7: Enzyme activity of bacterial isolates.

Sl. No.	Bacterial strain	Enzyme activity	
		Tannase	Laccase
1	AMETH 1	-	-
2	AMETH 2	-	-
3	AMETH 3	-	-
4	AMETH 4	-	-
5	AMETH 5	-	-
6	AMETH 6	-	-
7	AMETH 7	-	-
8	AMETH 8	-	-
9	AMETH 9	-	-
10	AMETH 10	-	-
11	AMETH 11	-	-
12	AMETH 12	-	-
13	AMETH 13	-	-
14	AMETH 14	-	+
15	AMETH 15	-	+
16	AMETH 16	-	-
17	AMETH 17	-	-
18	AMETH 18	-	-
19	AMETH 19	-	-
20	AMETH 20	-	-
21	AMETH 21	-	-
22	AMETH 22	-	-
23	AMETH 23	-	-
24	AMETH 24	-	-
25	AMETH 25	-	-
26	AMETH 26	+	-
27	AMETH 27	-	-
28	AMETH 28	-	-
29	AMETH 29	-	-
30	AMETH 30	-	-
31	AMETH 31	-	-
32	AMETH 32	-	-
33	AMETH 33	-	-
34	AMETH 34	-	-
35	AMETH 35	+	-
36	AMETH 36	-	-
37	AMETH 37	-	-
38	AMETH 38	-	-
39	AMETH 39	-	-
40	AMETH 40	-	-
41	AMETH 41	-	+
42	AMETH 42	-	+
43	AMETH 43	-	+
44	AMETH 44	-	+
45	AMETH 45	-	+

46	AMETH 46	-	+
47	AMETH 47	-	+
48	AMETH 48	-	+
49	AMETH 49	-	+
50	AMETH 50	-	+
51	AMETH 51	-	+
52	AMETH 52	-	-
53	AMETH 53	-	-
54	AMETH 54	-	-
55	AMETH 55	-	-
56	AMETH 56	-	-
57	AMETH 57	-	-
58	AMETH 58	-	-
59	AMETH 59	+	-
60	AMETH 60	-	-
61	AMETH 61	+	-
62	AMETH 62	+	-
63	AMETH 63	+	-
64	AMETH 64	-	-
65	AMETH 65	-	+
66	AMETH 66	-	-
67	AMETH 67	-	+
68	AMETH 68	-	+
69	AMETH 69	-	+
70	AMETH 70	-	+
71	**AMETH 71**	+	+
72	**AMETH 72**	+	+
73	**AMETH 73**	+	+
74	**AMETH 74**	+	+
75	**AMETH 75**	+	+
76	**AMETH 76**	+	+
77	**AMETH 77**	+	+
78	**AMETH 78**	+	+
79	**AMETH 79**	+	+
80	AMETH 80	-	+
81	AMETH 81	-	-
82	AMETH 82	+	-
83	**AMETH 83**	+	+
84	**AMETH 84**	+	+

+ Positive

- Negative

Table 8: Percentage of dye decolorization by selected bacterial strains.

Strain	% decolorization of RB81	% decolorization of RR111	% decolorization of RY44
AMETH 71	67.01	31.93	5.72
AMETH 72	94.17	66.36	16.40
AMETH 73	94.13	34.50	9.10
AMETH 74	17.9	14.30	1.81
AMETH 75	90.85	31.15	13.69
AMETH 76	93.44	60.53	10.68
AMETH 77	93.65	62.94	16.33
AMETH 78	86.36	28.59	13.62
AMETH 79	11.53	27.88	13.54
AMETH 83	5.66	12.52	13.47
AMETH 84	85.97	11.81	13.47

9 APPENDIX 2

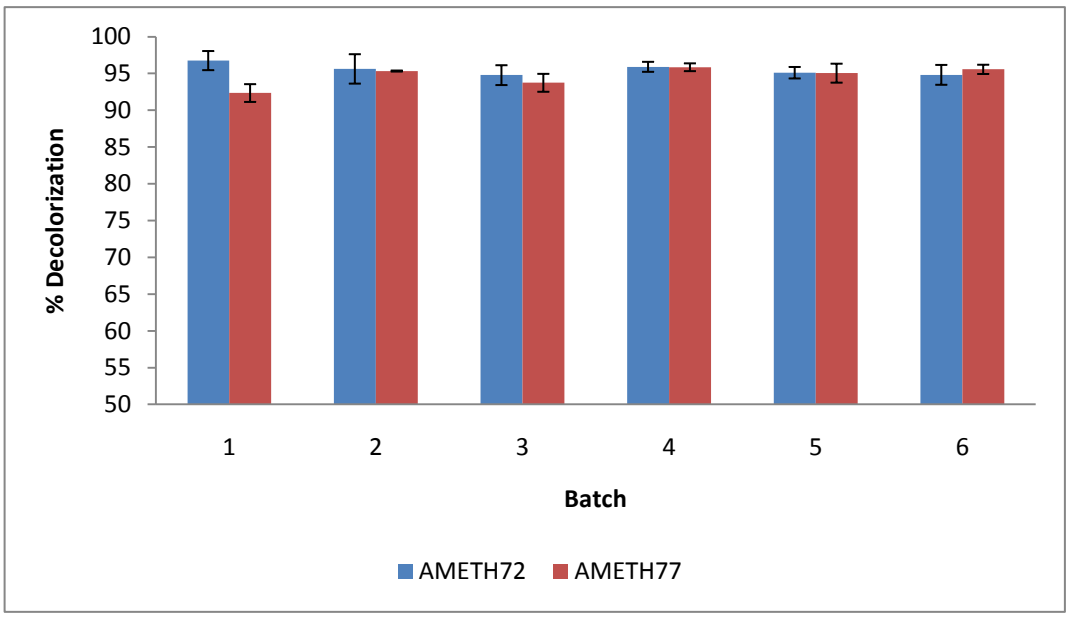

Fig 9.1: Decolorization percentage of RB81 by immobilized AMETH72 and AMETH77 (1bead/ml) in different batches.

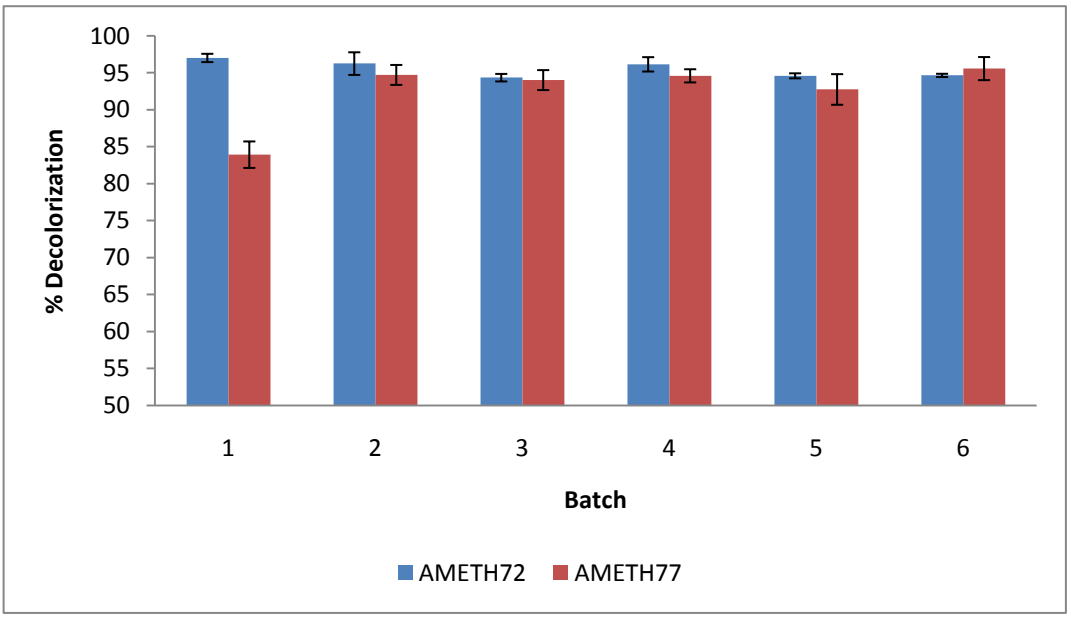

Fig 9.2: Decolorization percentage of RB81 by immobilized AMETH72 and AMETH77 (2beads/ml) in different batches.

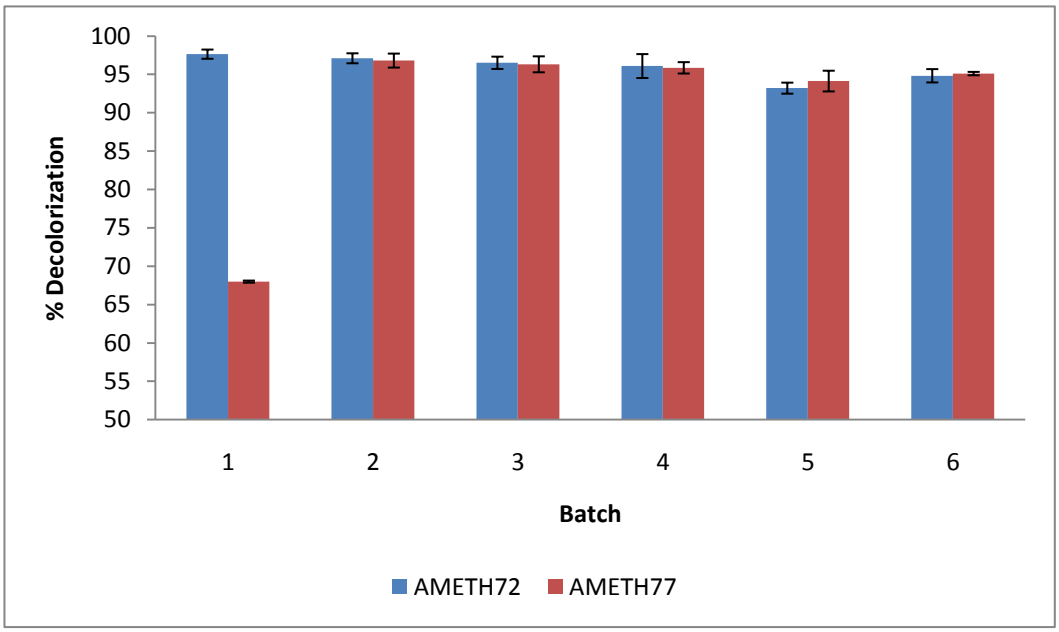

Fig 9.3: Decolorization percentage of RB81 by immobilized AMETH72 and AMETH77 (3beads/ml) in different batches.

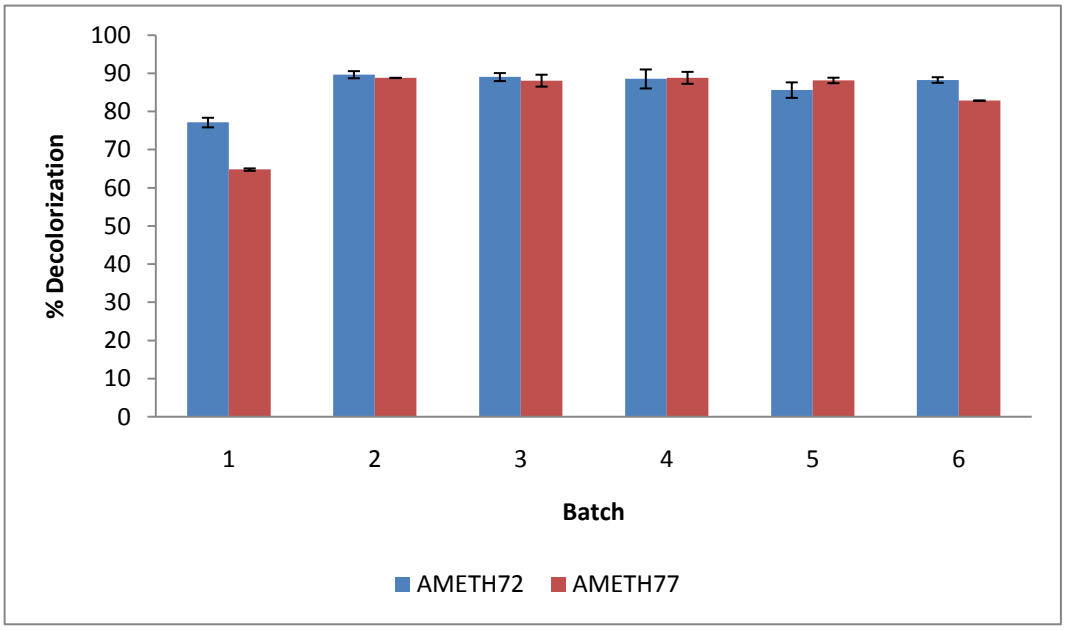

Fig 9.4: Decolorization percentage of RR111 by immobilized AMETH72 and AMETH77 (1bead/ml) in different batches.

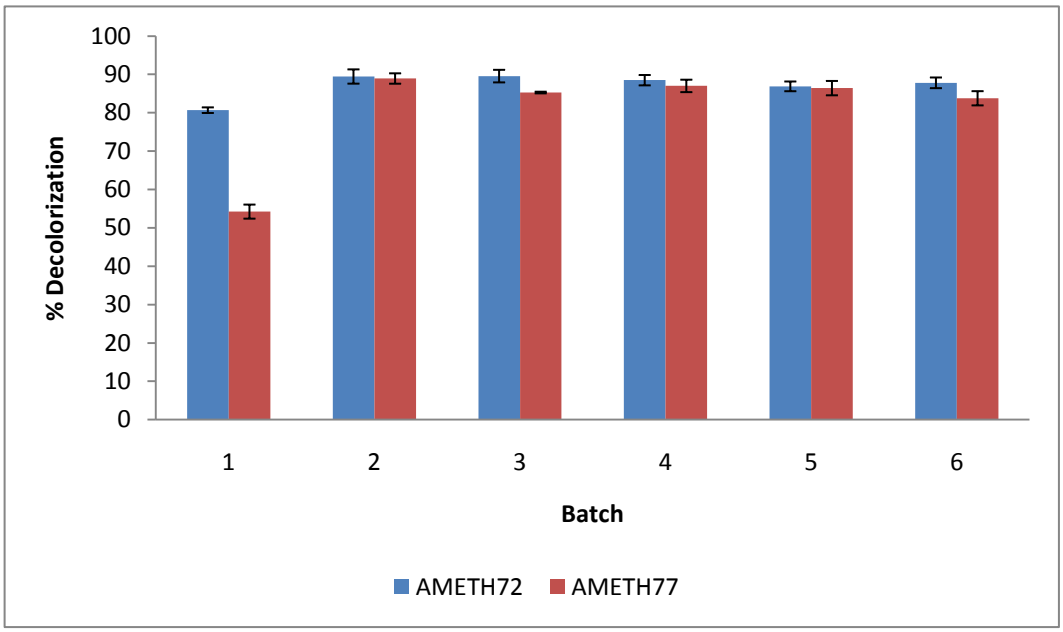

Fig 9.5: Decolorization percentage of RR111 by immobilized AMETH72 and AMETH77 (2beads/ml) in different batches.

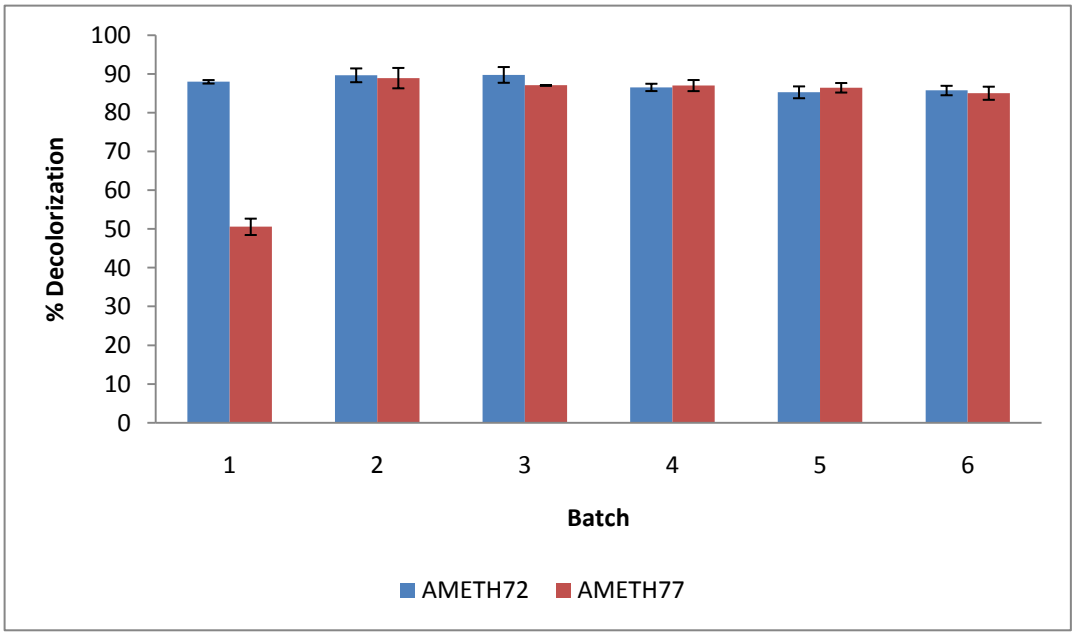

Fig 9.6: Decolorization percentage of RR111 by immobilized AMETH72 and AMETH77 (3beads/ml) in different batches.

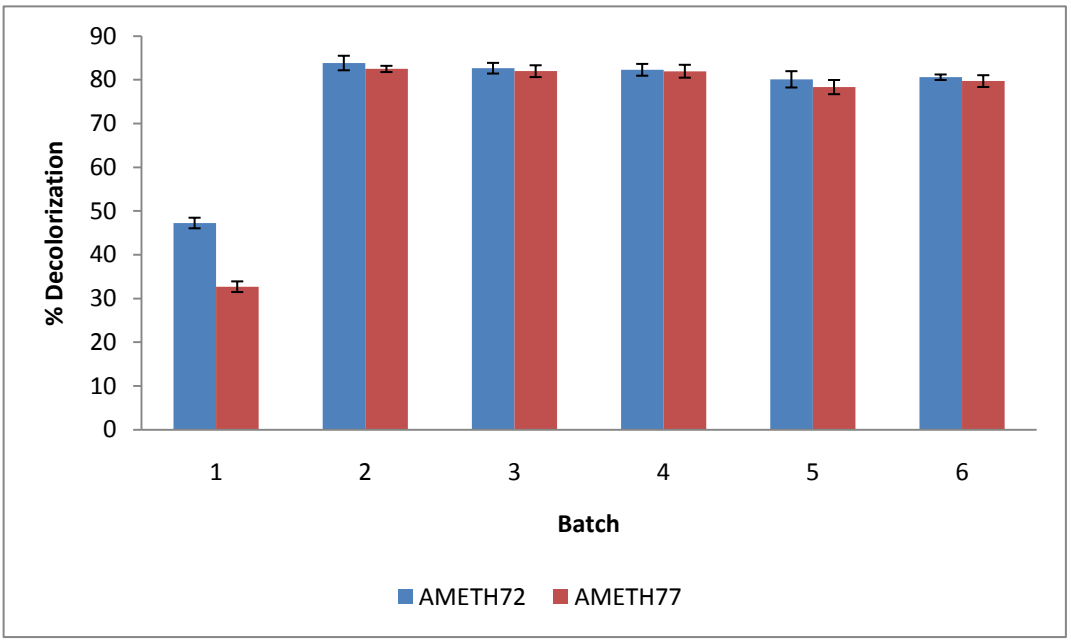

Fig 9.7: Decolorization percentage of RY44 by immobilized AMETH72 and AMETH77 (1bead/ml) in different batches.

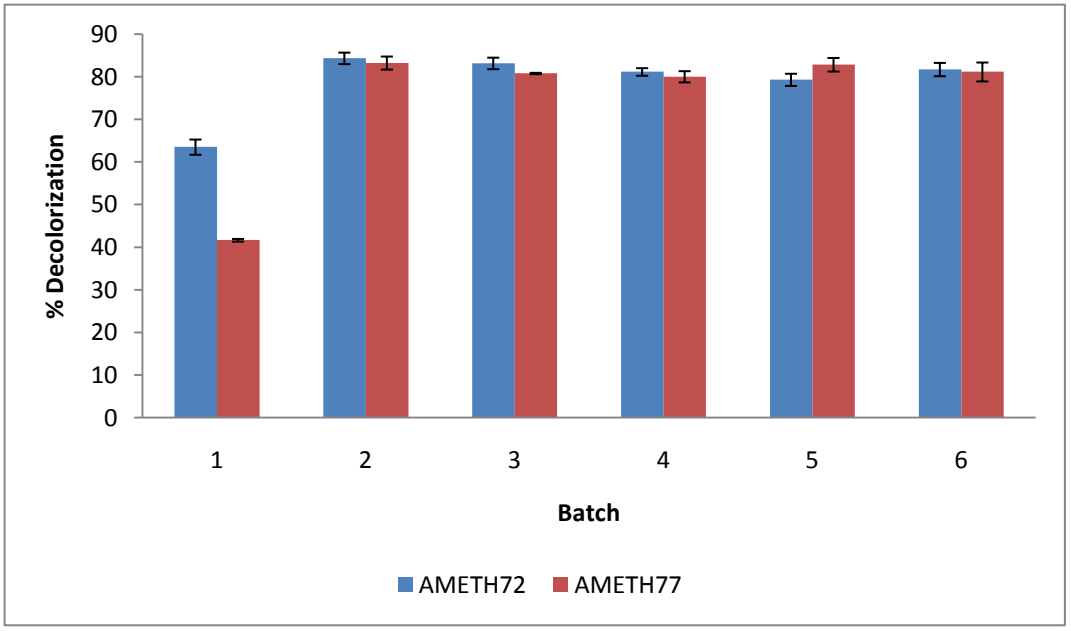

Fig 9.8: Decolorization percentage of RY44 by immobilized AMETH72 and AMETH77 (2bead/ml) in different batches.

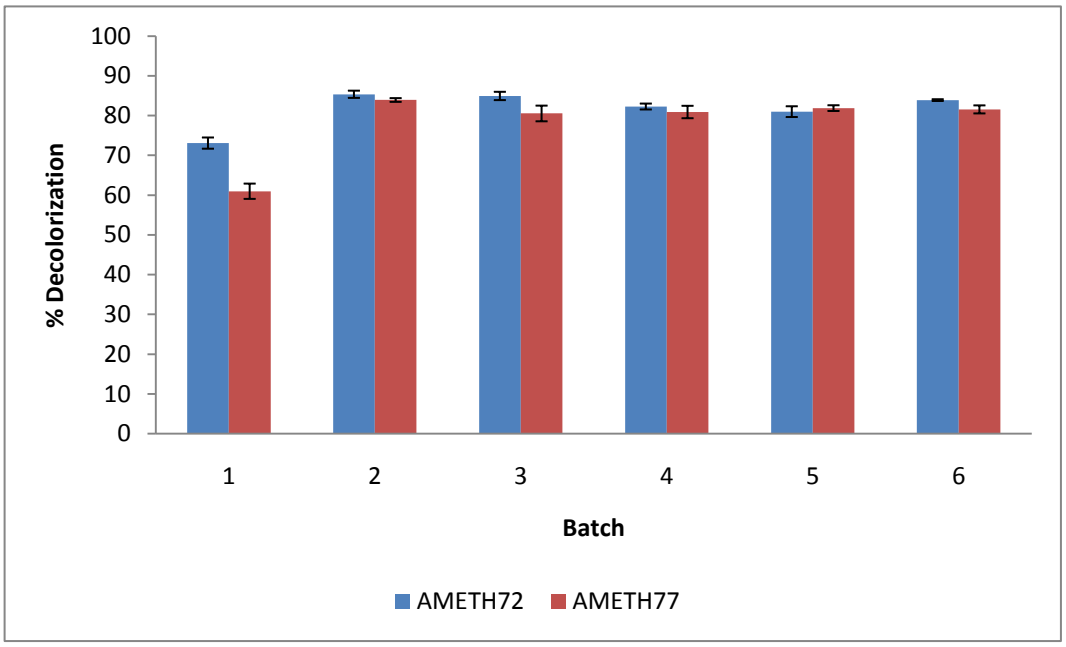

Fig 9.9: Decolorization percentage of RY44 by immobilized AMETH72 and AMETH77 (1bead/ml) in different batches.

10 APPENDIX 3

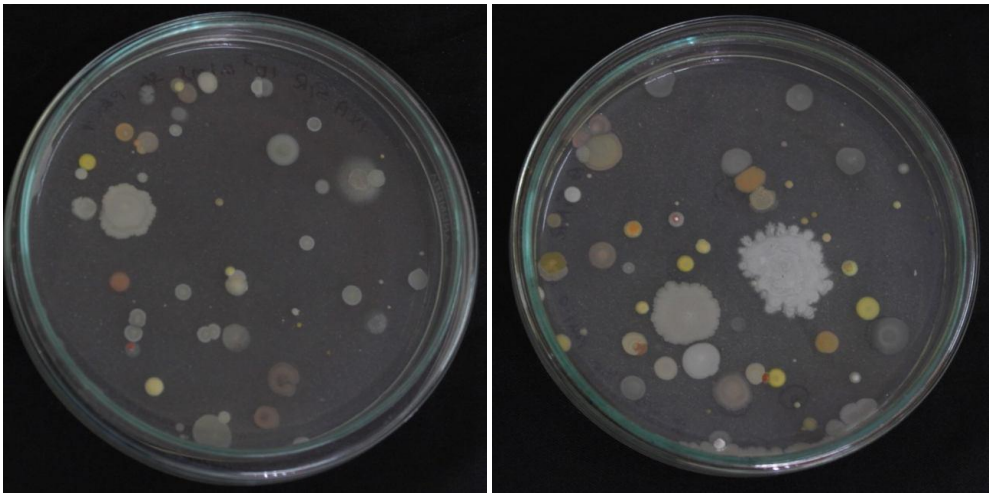

Fig 10.1: Isolation plates showing halotolerant bacteria from saltern soil samples.

.

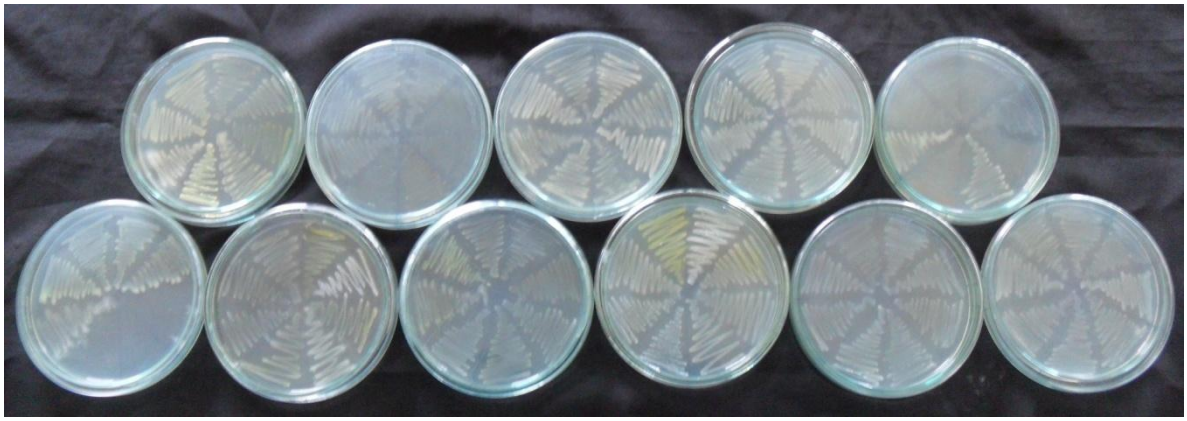

Fig 10.2: Pure cultures of halotolerant bacteria isolated from saltern soil samples.

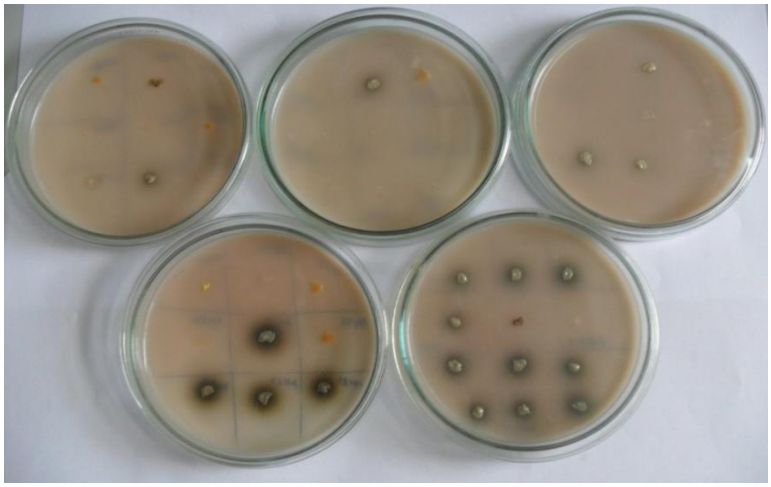

Fig 10.3: Halotolerant bacteria showing tannase enzyme activity (dark brown color zone).

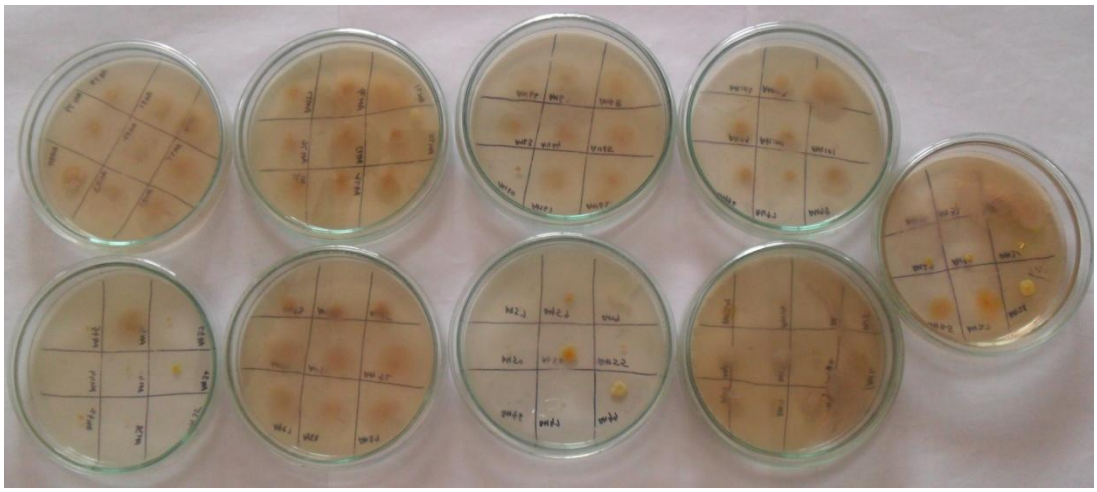

Fig10.4: Halotolerant bacteria showing laccase enzyme activity (reddish- brown coloration).

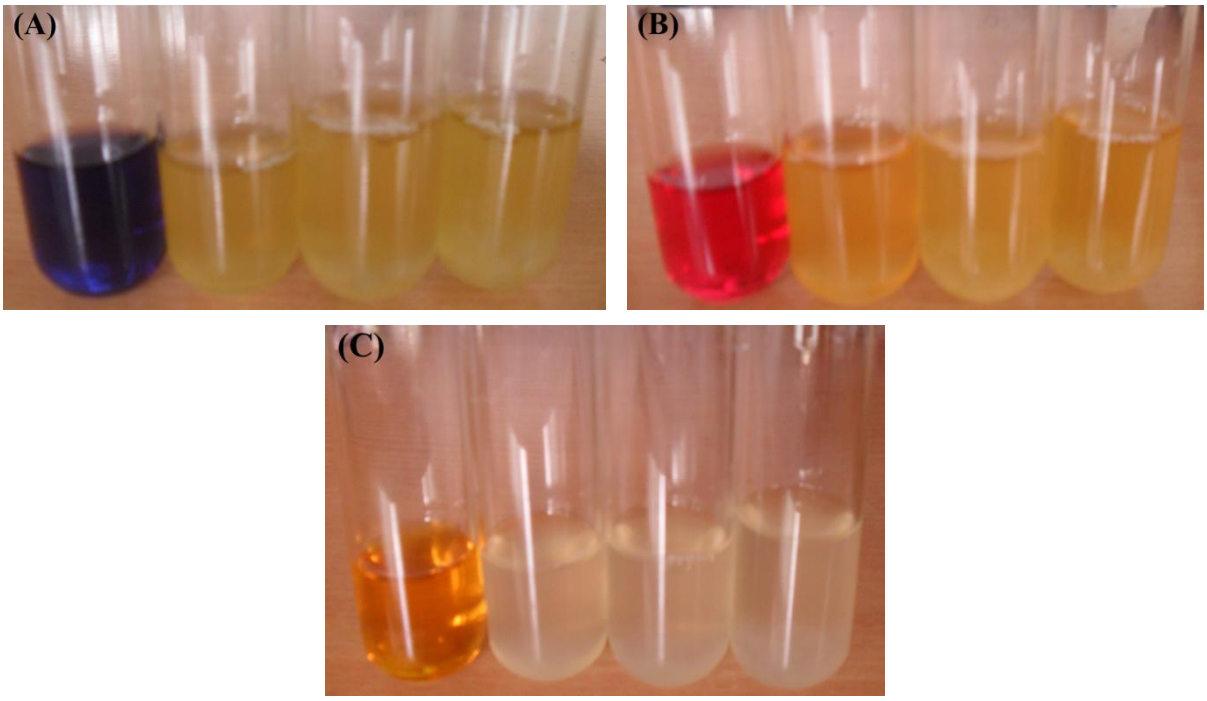

Fig 10.5: Decolorization of (A) RB81 (B) RR111 (C) RY44 by AMETH72 with varying number of beads (1 bead/ml, 2 beads/ml, 3 beads/ml).

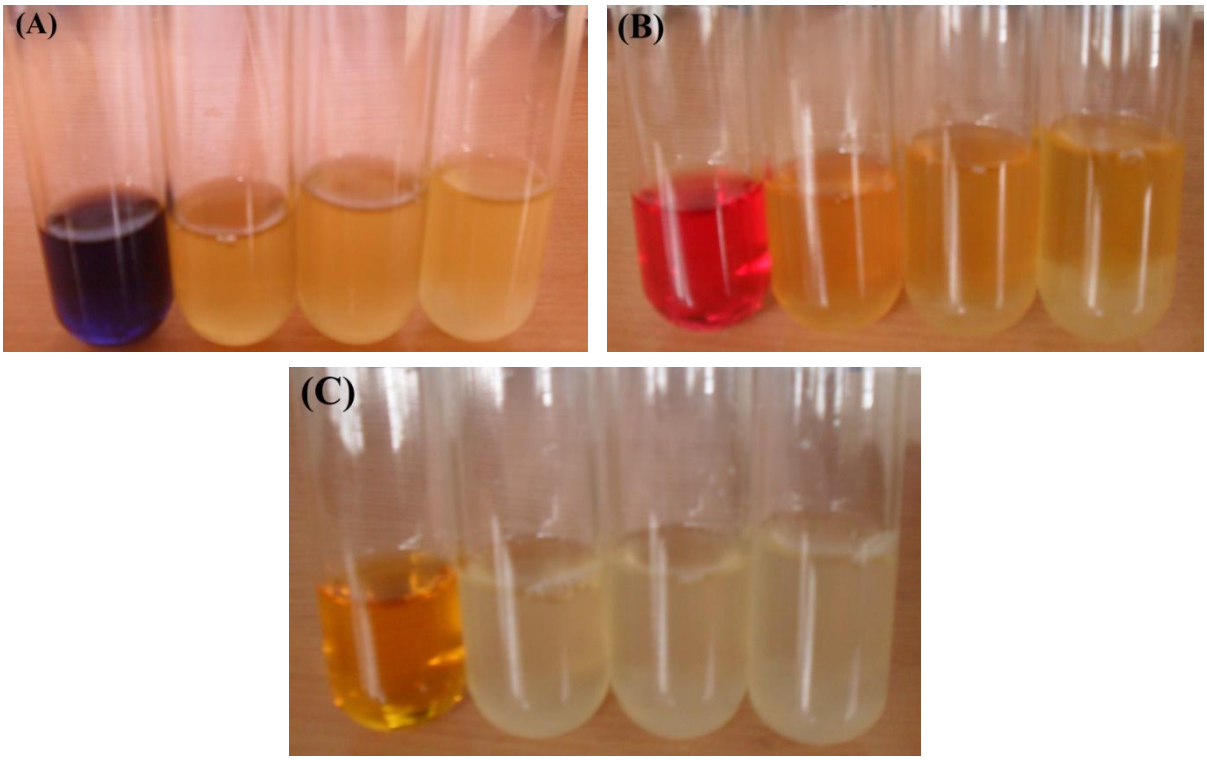

Fig 10.6: Decolorization of (A) RB81 (B) RR111 (C) RY44 by AMETH77 with varying number of beads (1 bead/ml, 2 beads/ml, 3 beads/ml).

Fig 10.7: Azo dyes from left RB81, RR111 and RY44 before (A) and after (B) degradation by AMETH72 (2 replicates shown).

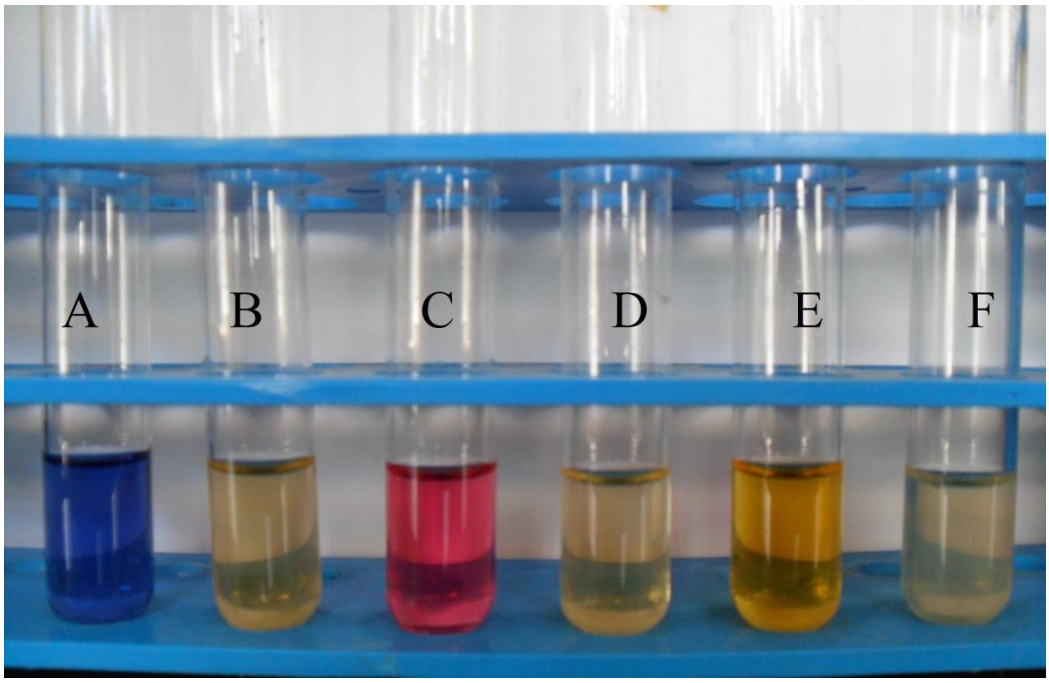

Fig 10.8: Decolorization of RB81, RR111 and RY44 by immobilized AMETH72. (A) Untreated RB81; (B) Treated RB81; (C) Untreated RR111; (D) Treated RR111; (E) Untreated RY44; (F) Treated RY44

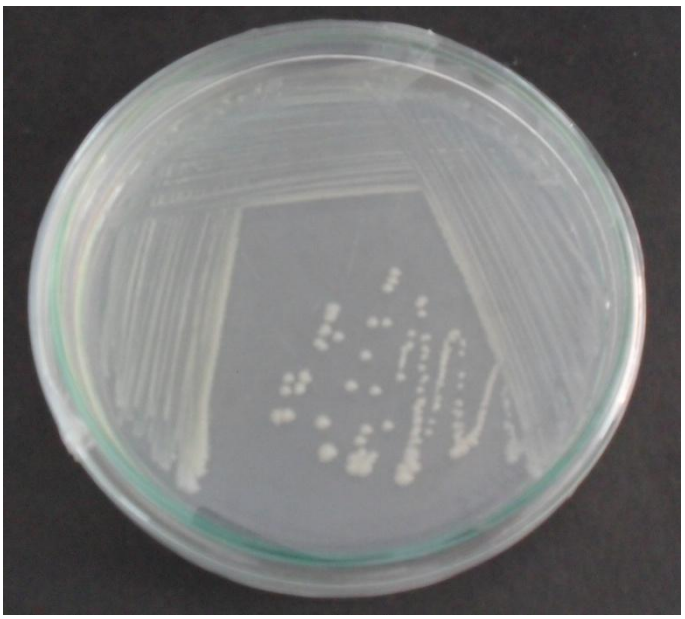

Fig 10.9: Pure culture of AMETH72 on 3% HA medium.

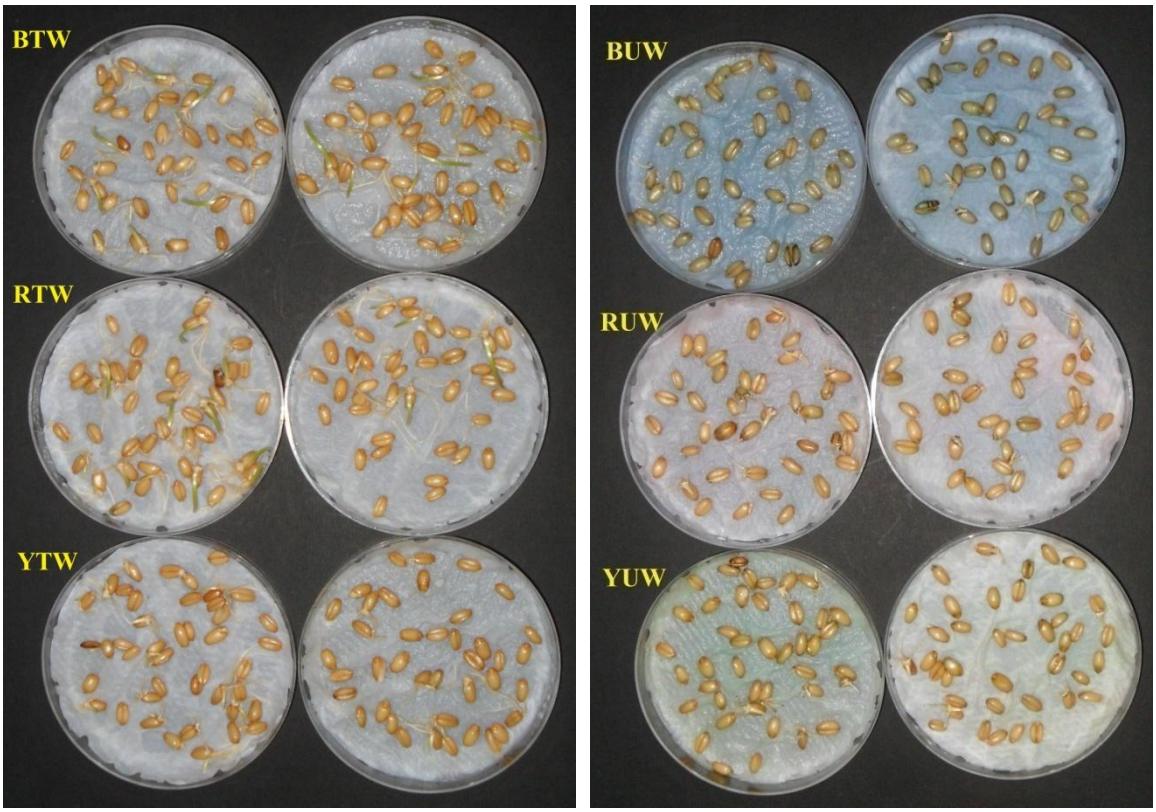

Fig 10.10: Effect of treated and untreated azo dyes on germination of Wheat seeds (2 replicates shown).

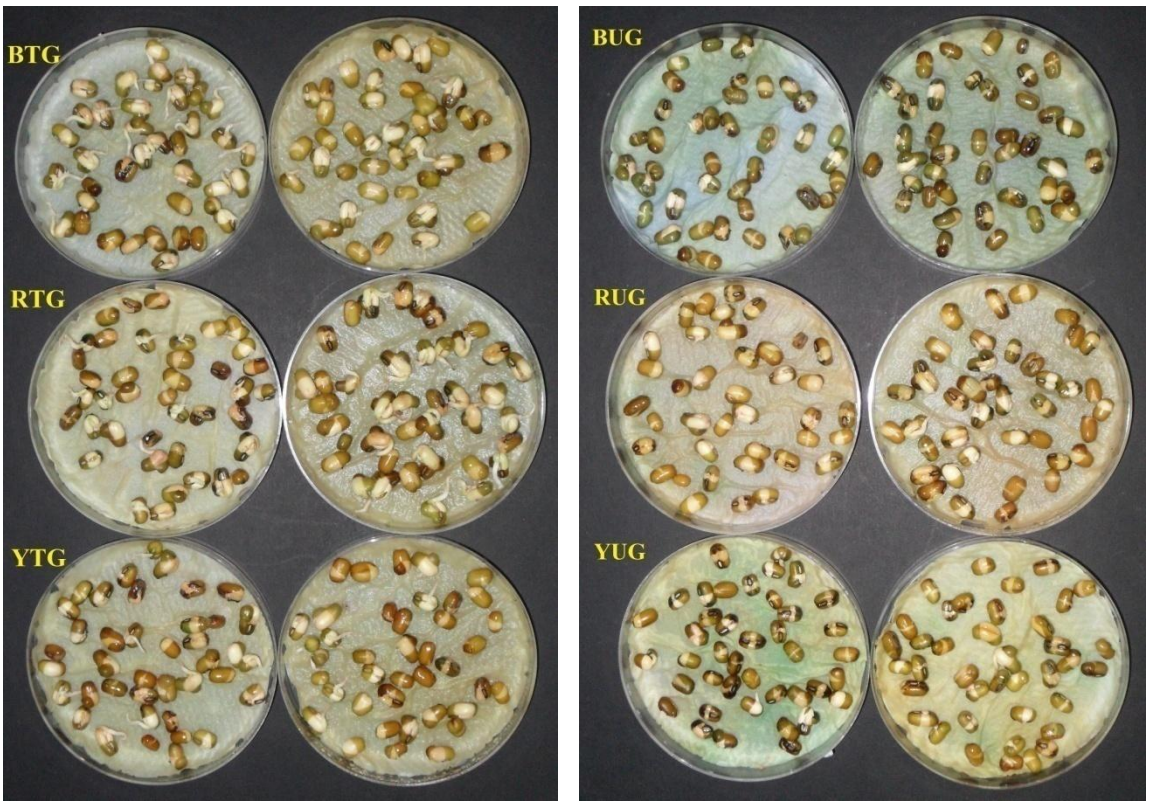

Fig 10.11: Effect of treated and untreated azo dyes on germination of Green gram seeds (2 replicates shown).

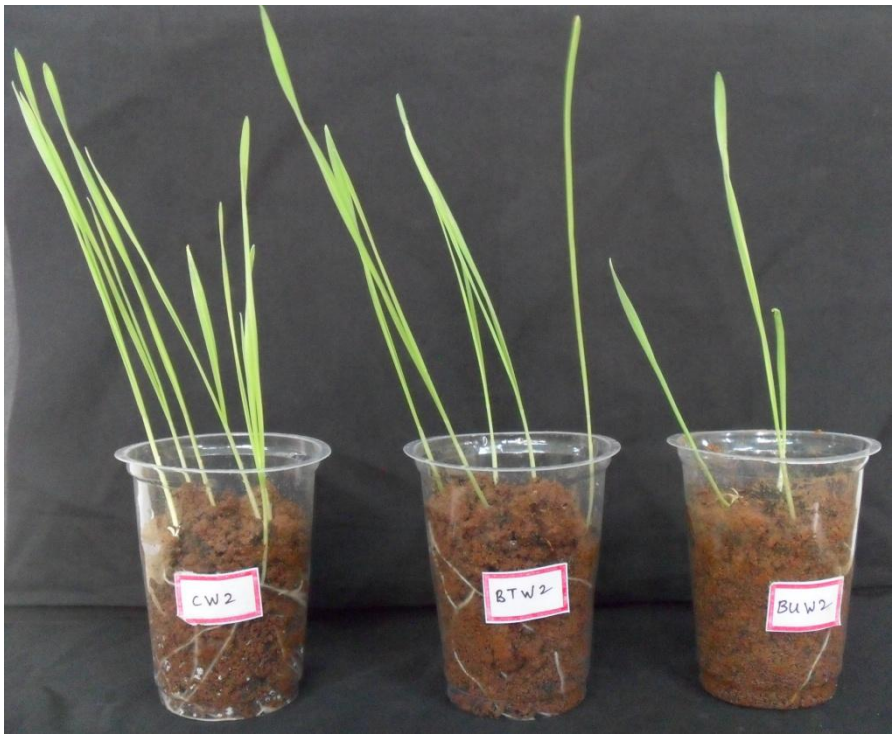

Fig 10.12: Effect of treated and untreated RB81 dye on the growth of wheat seedlings (from left CW, BTW, BUW).

Fig 10.13: Effect of treated and untreated RR111 dye on the growth of Green gram seedlings (from left CG, RTG, RUG).